2017

Target Read Operation of Passive Ultra High Frequency RFID Tag in a Multiple Tags Environment

Zi Qin Phua
University of Kentucky, ziqin.p@uky.edu
Author ORCID Identifier:
http://orcid.org/0000-0002-4204-4787
Digital Object Identifier: https://doi.org/10.13023/ETD.2017.031

STUDENT AGREEMENT:

I represent that my thesis or dissertation and abstract are my original work. Proper attribution has been given to all outside sources. I understand that I am solely responsible for obtaining any needed copyright permissions. I have obtained needed written permission statement(s) from the owner(s) of each third-party copyrighted matter to be included in my work, allowing electronic distribution (if such use is not permitted by the fair use doctrine) which will be submitted to UKnowledge as Additional File.

I hereby grant to The University of Kentucky and its agents the irrevocable, non-exclusive, and royalty-free license to archive and make accessible my work in whole or in part in all forms of media, now or hereafter known. I agree that the document mentioned above may be made available immediately for worldwide access unless an embargo applies.

I retain all other ownership rights to the copyright of my work. I also retain the right to use in future works (such as articles or books) all or part of my work. I understand that I am free to register the copyright to my work.

REVIEW, APPROVAL AND ACCEPTANCE

The document mentioned above has been reviewed and accepted by the student's advisor, on behalf of the advisory committee, and by the Director of Graduate Studies (DGS), on behalf of the program; we verify that this is the final, approved version of the student's thesis including all changes required by the advisory committee. The undersigned agree to abide by the statements above.

Zi Qin Phua, Student

Dr. Johné M. Parker, Major Professor

Dr. Haluk E. Karaca, Director of Graduate Studies

Target Read Operation of Passive Ultra High Frequency RFID Tag in a Multiple Tags Environment

---

THESIS

A thesis submitted in partial
fulfillment of the requirements for
the degree of Master of Science in
Mechanical Engineering in the
College of Engineering at the
University of Kentucky

By
Phua, Zi Qin
Lexington, Kentucky

Director: Dr. Johné M. Parker, Professor of Mechanical Engineering
Lexington, Kentucky 2017

ABSTRACT OF THESIS

Target Read Operation of Passive Ultra High Frequency RFID Tag
in a Multiple Tags Environment

Passive ultra-high frequency (UHF) radio frequency Identification (RFID) has emerged as a promising solution for many industrial applications. Passive UHF systems are relatively inexpensive to implement and monitor, as no line of sight is required for the communication. There are several advantages to using a passive RFID system. For example, no internal power source is required to activate the tags, and lower labor costs and efficient multitasking operations are expected in a long term scenario. However, due to factors such as tag-to-tag interference and inaccurate localization, RFID tags that are closely spaced together are difficult to detect and program accurately with unique identifiers. This thesis investigates two main ways to enable and improve multi-tag operations: physical tag placement and design of the near-field RFID reader antenna. First, several factors that affect the ability to encode a specific tag with unique information in the presence of other tags are investigated, such as reader power level, tag-to-antenna distance, tag-to-tag distance and tag orientation. A Full Factorial Design is carried out to study the effects of each of the factors and factor interactions. Results suggest a preliminary minimum tag-to-tag spacing which enables the maximum number of tagged items to be uniquely encoded without interference. In order to individually read each tag in a multi-tag form, an experimental device is built to enable controlled movement and positioning of the reader's antenna to the location of each of the tags. The experimental device is also designed to test other mechanical means of isolating the tags, such as shielding and mechanical isolation of the tagged media. Furthermore, to test a second method of improving the efficacy of programming tags uniquely in a multi-tag environment, the reader's antenna is redesigned to confine the electromagnetic field distribution to reduce the probability of activating non-targeted tags in the surrounding. Using the commercial software package ANSYS™ High Frequency Structural Solver (HFSS), the coupling interaction between the reader's antenna and RFID tags was simulated to investigate the relative voltage induced in the target tag relative to each of the proximal tags.The new antenna is then fabricated and validated with the simulation results. With a

better antenna design and ideals tag placement, the read operation of multiple tags can be improved and made more reliable. These findings can potentially expedite the process of field programming in item-level tagging and increase the throughput rate of unique tag encoding.

KEYWORDS: UHF RFID tags, Antenna design, Multiple passive RFID tags, Tag-to-tag interference, HFSS Simulation, Near-field antenna

Author's signature: Phua, Zi Qin

Date: February 28, 2017

Target Read Operation of Passive Ultra High Frequency RFID Tag
in a Multiple Tags Environment

By
Phua, Zi Qin

Director of Thesis: Dr. Johné M. Parker

Director of Graduate Studies: Dr. Haluk Karaca

Date: February 28, 2017

Dedicated to my family and friends. An utmost gratitude to my loving parents for their constant support and encouragement. I am thankful to the support and guidance provided by my graduate advisor, Dr. Johné M. Parker.

ACKNOWLEDGMENTS

This research was partially supported by Lexmark International, Inc. We thank our colleagues, Donnie Proffitt, Jason Hale, Robby Whitesell, Brandon Reynold and John Fessler from Lexmark who provided guidance and expertise that greatly assisted the research. We are also grateful to firmware engineer Mark Underwood for assistance in programming the test setup. I thank Flyod Taylor from the machine shop in University of Kentucky who assists us in the fabrication of the experimental device. Special thanks to Dr. David Herrin, Dr. Bill Smith and my advisor for being my final examination's committee members.

TABLE OF CONTENTS

LIST OF FIGURES

LIST OF TABLES

Chapter 1 Introduction

With a network of devices that does not require an active power source and is virtually maintenance free, the coverage of a communication system can be vastly widened without increasing cost and manpower. [33] This is the reason that Radio Identification (RFID) systems become increasingly important. They serve as the foundational technology to the Internet of Thing (IoT). Because of its exploding growth, the IoT has rapidly, yet steadily becomes an emerging technology that has the potential in revolutionizing operations and management especially in the industrial sectors. [35]

1.1 Purpose

Although the benefits of RFID technologies are very promising, there are certain areas that RFID systems will not perform as expected. Specifically, in a near field environment, many closely spaced passive Ultra High Frequency (UHF) RFID tags will affect the readability and programming rate of the tags. This effect is known as tag-to-tag interference/collision. There are also external factors like environmental effect which can possibly detune the transmitting antenna. One of the objectives at the RFID lab of University of Kentucky was to investigate the ideal parameters to program a variety of RFID tags. [18, 23] Since 2008, multiple form factors of tags have been tested in various configurations to study the performance of the RFID system.

As an extension of previous work, this thesis aims to investigate the possibility of a controlled multiple passive tag operation in a relatively compact space using a single antenna. When we transition from a single tag operation to a closely spaced multiple tags operation, the effect of tag-to-tag interference to the readability of a targeted UHF RFID tag becomes more prominent. Hence, experimental investigation was carried out to find the optimum UHF RFID tags placement on a media that will yield an effective multiple tags programming operation. We were also investigating how different materials affect RF waves propagation (in our custom experimental setup) and ways to mitigate its effect in a near-field application.

To further increase the efficacy of programming operation, a new antenna (designated as "Merida") is designed and compared to the prior antennas used in the setup. Simulation using ANSYS™ High Frequency Structure Solver (HFSS) was completed to compare the measured characteristics of the antennas we used. Certain changes were recommended in the simulated models to increase the readability in tags crowded environment. These findings can significantly speed up the process of field programming in item-level tagging.

1.2 Research Questions

Based on the purpose and motivation explained above, we designated two main research questions to be investigated in this thesis.

1. What is the optimal tag configuration that produces the highest UHF RFID target tag readability in a multiple tags near-field system?
    a) Assumptions: The targeted stationary RFID tag is directly positioned under the center of antenna. By varying all the factors, we will be able to only detect the target tag using a combination of ideal parameters.
    b) Limitations: To prevent detection of surrounding non-targeted tags, the readability of targeted tags will be lower compared to a single tag operation. Detection of non-targeted tags is undesirable under most circumstances. Performances may vary across different type of tags.
2. Which antenna design helps to reduce the cross-activation of surrounding non-targeted tags?
    a) Assumptions: A strong, confined magnetic field so that only a single RFID tag in the specific direction can be activated. Its readability would be relatively higher because of the confined field illuminated on the target tag compared to previous antennas under the same parameters.
    b) Limitations: Antennas must be relatively small in size to be fitted in an enclosed space and be able to overlap just a single RFID tag. The fabrication process must not be overly complex.

1.3 Thesis Structure

The first chapter of the thesis gives an introduction to the importance of RFID technologies. A brief history and its advantages are also discussed. We present the research questions and some its assumption and limitations. The second chapter gives a comprehensive review to the background and working concept of RFID systems. Relevant literature relating to tag-to-tag interference, environmental effects, antenna studies and relevant governing equations are also discussed. The third chapter gives an overview of methodology, tools and equipment employed in the experiments.

The fourth to sixth chapters discuss and address the two research questions raised in this thesis, including the results and analysis of the experiments. Various factors and their significance that affect the readability are discussed in the fourth chapter. The custom built experimental device is also explained in detail in the fifth chapter. Experimental data and simulation results are compared in each relevant section. The

sixth chapter looks into the simulation and design of the specific antenna for our application. The last chapter concludes the research questions in the thesis and presents the potential contribution of this research, including future work and limitations.

1.4 Brief History of RFID Technology

An effective combination of communication systems is central to a civilized society. Technologies in communication have evolved from physical signals (like smoke and sound) to small portable hand-held devices. These devices were developed initially as separate networks for individual purposes. [11] However, as the drive for connectivity grows, devices from different systems are linked together to provide a reliable and extensive communication. It is the versatility and simplicity of RFID systems that enable the technology to be deployed in various sectors, whether it is industrial, systems monitoring or security. [19] Hence, RFID has gained a significant amount of interest in recent years.

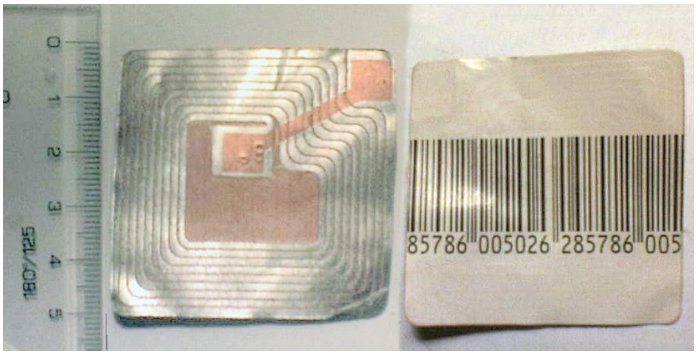

Figure 1.1: RFID tag with barcode printed on the back (Kriplozoik 07)

The invention of RFID technology dates back to World War II. A Soviet Union scientist, named Léon Theremin created a covert listening device that could be powered by radio waves. Even though it was only a listening device, the device was essentially a long-range passive RFID tag. [21] In the 1940's, the Allies were developing a similar ID tracking device to monitor the incoming airplanes returning to the base. A Scottish physicist, Sir Robert Alexander Watson-Watt, invented an active identify friend or foe (IFF) system. Planes were equipped with a radio transmitter which would respond back to the signal broad-casted by the ground radar stations. [27] Since then, several advancements hav been made to improve the tracking system and expand its usage to a wide variety of applications.

The major advantage of an RFID system is that it does not require a line of sight to access information. At the same time, many unique tags can be detected in a relatively short span of time without additional manual work. [34] Figure 1.1 shows a tag with bar code printed on the back. This has the benefit of visual tagging and RF tagging if the tag is not visible. Hence, a tagged item can be tracked with real

time notification, and unattended inventory is more efficiently monitored. When the on-site supplies or goods are out of stock, the employer can be notified automatically instead of manual tracking, saving time and labor cost.

Table 1.1: Companies adopting RFID technologies and their primary objectives (Data sourced from RFID Journal & Roh, Kunnathur, and Tarafdar [28])

Company	**Applications for RFID Adoption**
Wal-mart	To track the inventory of its products more effectively
Intel Corp.	To increase efficiency in supply chain and decrease delivery time
Johnson Control	To minimize human error in checking and delivery
Metro Group	To encourage modernization process in commerce
Paramount Farms	To increase efficiency of harvest management
NYK Logistics	To improve throughput of containers at its distribution center, Long Beach, CA

The number of research and journal publications in the field of RFID technology and applications has increased due to its advantages over conventional tracking methods (like printed ID). In the meantime, more industries are seeking and adopting the RFID option in order to save operational costs and enable multitasking of applications. [20] According to a report from RFID Journal, there was a huge rise in the global sale of UHF Gen 2 chips by more than 200 percent in 2010 compared to the prior year. [32] Some industries, listed in Table 1.1, have shown positive adoption results in integrating the RFID technology in daily operations. [28]

Chapter 2 Literature Review

In this chapter, we present the basic functioning principle of the RFID technology. We will also focus on some of the principles and governing equations behind the primary components in a RFID system. With a thorough foundation on the working principle, we have a better understanding of the pros and cons of choosing the factors and components for our setup. Various literature is reviewed and discussed in relation to the research questions. Specific literature on UHF antenna design is also reviewed in later chapters.

2.1 Functioning Principle of RFID System

RFID technologies evolve based on our understanding in electromagnetic energy studies, which traces its roots back to the explanation of Electromagnetic (EM) waves Duality by English Scientist, Michael Faraday. [15] In recent decades, the improvement of semiconductor technology has allowed cheaper manufacturing, increased reliability and performance. As a result, this gave a huge boost to the industrialization of RFID technologies. [13]

Radio waves can be separated into many categories; UHF RFID systems tend to sit in the bandwidth of 865 MHz to 954 MHz. Table 2.1 shows some of the most commonly used frequency bandwidths that are regulated by International Telecommunication Union (ITU). In general, UHF systems are suitable for item level tagging because of its increased data transfer rate and inexpensive implementation. For example, the ThingMagic™ M6e reader from Trimble claims to be able to achieve a tag read rate of 750 tags per second with the high performance setting. It means that the data on RFID tags can be accessed and stored at a quicker time with a better range than the lower frequency applications, hence, making it very ideal for supply chain management. [15]

Per regulations enforced by Federal Communication Commission (FCC), the frequency that UHF RFID operates in the USA is in the band of 902 - 928 MHZ. In addition, no license is required to operate the equipment. In order to prevent interference, the frequency is set to hop in the regional bandwidth usually at 0.4 seconds. [6]

Components of RFID system

In general, a RFID system consists of an antenna, reader and tags. Figure 2.1 shows the basic passive RFID tag system operation. The reader operation consists of a

Table 2.1: Radio Frequnecy Band and its Applications (Sourced from ISM ITU-R Radio Regulations)

Frequency	**Bandwidth**	**Application Examples**
Low Frequency (LF)	125 - 134 kHz	Identification in animals (Microchip)
High Frequency (HF)	13.56 MHz	Near Field Communication (NFC), Smart Cards, ePayment
Ultra High Frequency (UHF)	433 MHz	Amateur Radio, Radar (Defense)
	865 - 868 MHz	RFID in Europe and Middle East
	902 - 928 MHz	RFID in USA, Canada and Americas
	920 - 925 MHz	RFID in China, Thailand, Vietnam, Australia
	952 - 954 MHz	RFID in Japan
Microwave Frequency	2.45 - 5.8 GHz	IEEE 802.11 (Wi-Fi), Bluetooth, Cooking Appliance
	3.1 - 10 GHz	High Speed Communication in PC peripherals

radio and antenna, sending out a radio signal, which powers the tags. Once the tag is activated, it generates a signal back to the RF system, and the signal is modulated to carry the information that was stored in it. This process is know as the backscatter, and this backscattering is detected and interpreted by the reader.

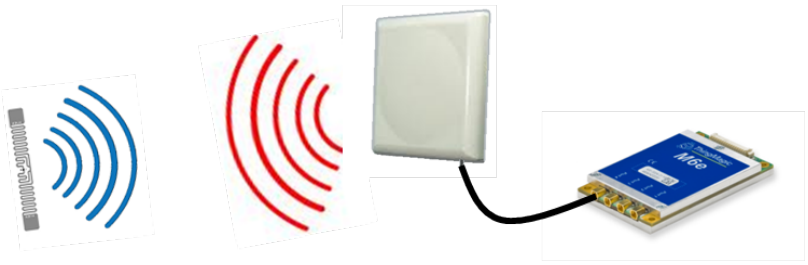

Figure 2.1: Major components of a passive RFID system

Type of tags

In general, RFID tags can be categorized into passive and active tags. The active RFID tag contains (a battery) or connects to a power source so that it can constantly

read and track over a certain distance. Hence, active tags can be differentiated from one another because they can each broadcast a unique beacon which can be detected over a much longer range.[34] Due to a complex inner circuitry, the active RFID tag is usually bigger in size, more costly and physically rugged compared to a passive tag, as shown in Figure 2.2. On the other hand, passive tags rely on the power captured from electromagnetic (EM) waves or magnetic induction. Hence, they are generally easier and more economical to manufacture, and since they contain no major moving parts. The trade-offs are lower memory capacities and a shorter read range.

Figure 2.2: Passive RFID tag and active RFID tag (atlasRFIDstore)

A typical passive RFID tag consists of a tag antenna, Integrated Circuit (IC) and substrate that holds all the components. They can vary in sizes, shapes and ICs to perform various operations. The basic structure of a passive tag is shown in Figure 2.3. The performance characteristics of RFID tags are generally categorized by the tag antenna and the IC types. Hence, they can sometimes be divided into far field and near field tags. The RFID tag coordinates the transfer of ID and information stored to the tag antenna while its structural integrity are maintained by its encapsulation. [34] The selection of tag type usually depends on the application and advantages of each tag type for that application

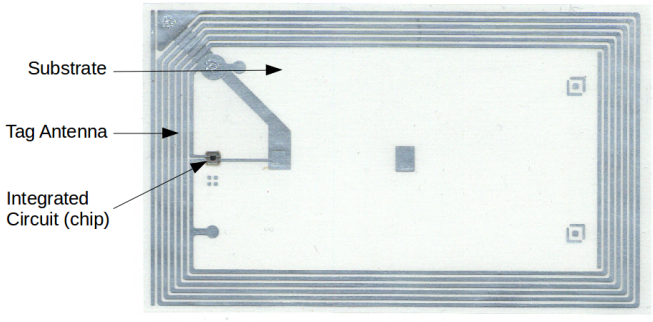

Figure 2.3: Basic components of a passive RFID tag (Dokkum R. V. 09)

2.2 Regions of Antenna System

The fundamental operating regions of an antenna system can be separated into two classes, namely near-field and far-field. This section is important to understand the basic electromagnetic characteristic of the different operating regions of an antenna. Free space impedance governs the relationship between these fields, and both attenuate over range of $1/r$ (where r is a separation between tag and reader).[22]

The Governing equations for separating the near field and far field boundary (λ = wavelength) [22]:

$$r = \frac{\lambda}{2\pi} \tag{2.1}$$

We can use Equation 2.1 for approximating boundary for antennas which has dimension closes to a wavelength.

$$r = \frac{2D^2}{\lambda} \tag{2.2}$$

Equation 2.2 is only applicable for electrically small antennas where D is the largest dimension of the particular antenna.

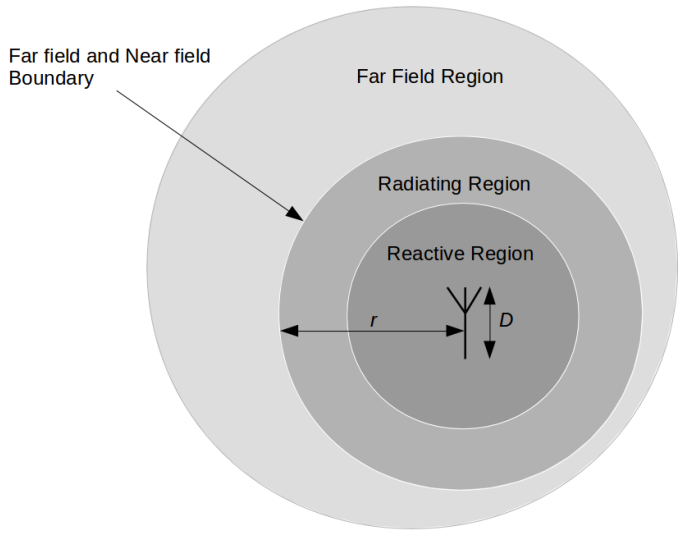

Figure 2.4: Near and far-field regions of an antenna with length D

In the far-field region, the tag captures EM waves emitted by the antenna and then produces a back-scatter signal that will be recaptured by the antenna. The main communicating mechanism for far field tags are through back-scattering. A precisely designed antenna can be tuned to a particular frequency. By actively changing the

impedance of this antenna (controlled by the IC), the RFID tags can emit a pattern of RF waves that can be decoded by the RF reader. This operating principle relies heavily on the sensitivity of the RF receiver. [34]

When the distance from the antenna is more than 2 wavelengths away, the Friss equation is used to calculate the ratio of power available of the receiving antenna, P_r to the power transmitted, P_t.

$$\frac{P_r}{P_t} = G_t\, G_r \left(\frac{\lambda}{4\pi R}\right)^2 \tag{2.3}$$

where G represents the gain of the receiver and transmitter, R is the separating distance.

As for the near-field region, this class can be further split into two different fields, which are reactive and radiating. It is the reactive region that is highly influenced by objects with higher dielectric properties. Such objects are powered by magnetic induction and they are generally suitable for item level tagging because of the short read range. The illustration of the regions is shown in Figure 2.4. Strength of magnetic field drops off at $1/r^3$ which is much faster than a far-field system. [34] Nikitin, Rao, and Lazar [22]also provided an explanation on four critical approaches in implementing near field UHF RFID using existing reader modules and tags.

For our particular system that operates in the UHF band in North America, the wavelengths in the region of 902 - 928MHz are calculated based on the equation below.

$$\lambda = \frac{v}{f} \tag{2.4}$$

where v represent the speed of the propagating wave. In this case, it is the speed of light, $c = 3 * 10^8$ m/s.

The boundary which separates the near field and far field region is located about 33 cm from the source. The reactive near field region starts at roughly 5.2 cm based on Equation 2.1, assuming a central frequency of 915MHz. Most of the experimental test in this thesis were conducted within the UHF near field region in our setup, which is well below 33 cm. Hence, most of the tags and antenna in our experiments were inductively coupled.

Classification of RFID System

Based on the understanding of specific operating regions of the antenna, we will discuss the advantages and disadvantages of each type of RFID system in this section. In general, the selection of each type of system largely depends on the application.

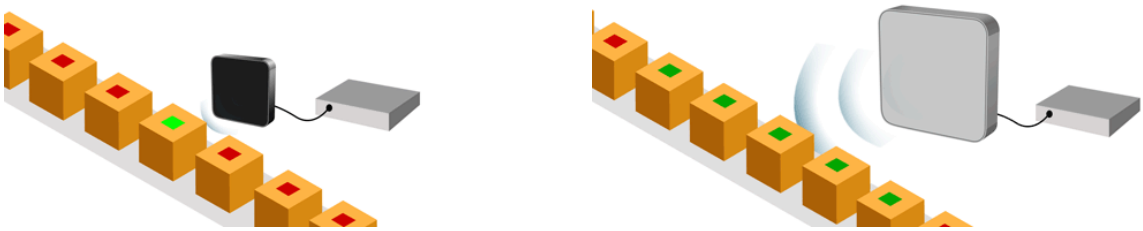

(a) Near Field RFID System (b) Far Field RFID System

Figure 2.5: Two major types of RFID systems (Source: atlasRFIDstore)

Since the field created by far field antenna system is not localized and it covers a bigger area over distance, more tags are usually detected in this case, shown in Figure 2.5b. Because of the dominance of the electric component in the far field system, they can also easily be affected or detuned by materials like metals or liquid. This effect will be further discussed in the next section. A sufficient understanding of this detuning effect is important to minimize the materials effects in the construction of our experimental device and our test results.

A near field system is usually intended for shorter range application and more suitable for precise item level tagging. As the magnetic field is more dominant in a near field system, a relatively small size near field antenna can be used to avoid activation of unintended tags, as shown in Figure 2.5a. Hence, partly due to this reason, we have chosen to employ a near field system in our setup for a better target tag control.

2.3 Effect of Material Properties on RF Wave Propagation

One of the most important aspects of passive RFID systems is the read range. There are several factors that affect the performance of RFID systems. One of them is the influence of material objects in close proximity or in placement between the tags and antenna. From a recent literature search, this area of RFID research has not been extensively explored. Most studies have investigated the substrate materials in constructing the antenna. [20] This section is particularly important because it helps us to establish the constraints in designing our new experimental device in Chapter 6.

In an industrial supply-chain scenario, tags are placed in multiple containers, possibly with different material in a general space. The tags' power and signal strength rely on EM waves; these can experience interference when the signal travels through

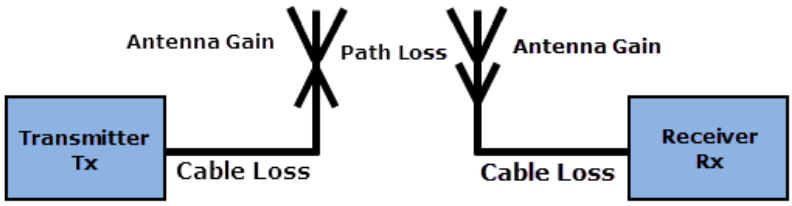

Figure 2.6: Path loss in a RF System

various materials. The total path loss can be broken down into loss in reflection, attenuation loss through materials and spreading loss, as illustrated in Figure 2.6. [8] Spreading loss is the basic transmission loss when they are no objects nearby or directly on the path of signal propagation. [29] Attenuation characteristics and reflection loss are governed by the dielectric constant of materials. [16]

The difference in dielectric constant (also known as relative permittivity) of materials influences the sensitivity of frequency and then restricts the reading of tags. Tabel 2.2 shows the dielectric constants of common materials at room temperature. In general, if the tags are in very close proximity on metal surface, it will suffer a significant decline in readability because of a higher dielectric constant. [7, 16] The reason was due to the induction of eddy current in the metal from the incident magnetic field. Magnetic flux generated by the antenna is then countered by the induced current. As a result, the antenna frequency is shifted substantially due to the variation of inductance. [24]

Table 2.2: Dielectric Constant of materials at room temperature (Sears, Zemansky, Young Table 27-1)

Material Types	**Dielectric Constant**
Air	1.005
Glass	5 - 10
Plexiglass	3.4
Water	80.4 (20 °C)
Paper	3.85
Wood	Highly dependent

For signal propagation through objects, reflection and transmission coefficients can be used to model the transmission loss through multi-layer objects. [8] In a study done

by Ali-Rantala, thickness of wooden materials does not affect attenuation because it is inherently an inferior conductor. However, for concrete and plaster (which has less attenuation than concrete), propagation loss is related to both antenna frequency and material thickness. [1]

For objects that have relatively thin thickness placed between the tag and reader, the gain of the tag antenna is relatively higher because of the lensing effect. Due to the detuning of antennas, tag antennas with a broad and flat impedance bandwidth are preferred when there are dielectric materials in close proximity. [30] Relatively thin materials, operating under CDMA frequency, like Lexan® Polycarbonate, Styrofoam™ polystyrene board and Tuff Span® fiberglass do not have significant attenuation effects on the signal propagation.

Laniel, Uysal, and Emond [14] conducted an experiment comparing different RF interactions with air cargo container. From their discussion on UHF frequency propagation, the aluminum sample had an increased signal strength when the receiving antenna was placed in between the transmitting antenna and sample. They also noted possible signal scattering (edge diffraction in particular) because the length of sample size is almost similar to the wavelength of UHF. Some materials also slightly reflected the signal when the receiver was located $\lambda/2$ in front of the sample.

By understanding the behavior of a RFID system and its signal propagation, its performance can be optimized by tweaking environmental objects based on the application. In addition, reflections and interferences are more influencing than absorption in liquid and dielectric materials. [8] In general, objects with high dielectric properties should not be placed in close proximity to the tags or antennas. Placement of tag antenna at location with maximum gain is preferred. [30] By overcoming some limitations, readability of tags in near-field region can be improved.

2.4 Theory

We present the fundamentals of Electromagnetism, especially in lossy medium and material attenuation.

In order to investigate this particular topic, our calculation end goal is to determine the final power absorbed by the RFID tag chip in the antenna coupling. This can be modeled as:

$$P_{chip} = P_{reader}\,\rho\,C\,\tau \tag{2.5}$$

where P_{reader} is the reader power output, ρ is the impedance matching coefficient between reader and transmitting antenna, τ is the impedance matching coefficient between tag IC and tag antennas, and lastly C is the coupling transmission loss.

Impedance matching coefficient can be calculated as [25] :

$$\rho = \frac{4\,R_r\,R_t}{|Z_r + Z_t|^2} \tag{2.6}$$

where Z_r is the reader impedance and Z_t is the transmitting antenna impedance.

Next, by combining the wave equations for lossy medium and the time-harmonic Maxwell's Equation, we can calculate the propagation constant in terms of the known material properties.

$$\nabla^2 E = j\omega\mu\sigma E - \omega^2\mu\epsilon E \tag{2.7}$$

$$\nabla^2 H = j\omega\mu\sigma H - \omega^2\mu\epsilon H \tag{2.8}$$

where

$$E, H \propto e^{j(\mathbf{k}\cdot\mathbf{r} - wt)}$$

Calculation of Transmission Constant

Fletcher, Marti, and Redemske [8] from the Auto-ID labs provided a good model for calculating the propagation loss through a material. These equations enabled us to predetermine the transmission constant for the materials we have selected.

First, we define the relationship between the dielectric constant (ϵ) and the effective conductivity (σ). The loss tangent ($\tan\delta$) is obtained. A lower loss tangent means the material has a lower dielectric loss.

$$\epsilon = \epsilon' - j\epsilon'' \tag{2.9}$$

$$\begin{aligned} \tan\delta &\equiv \frac{\epsilon''}{\epsilon'} \\ &= \frac{\sigma}{\omega\epsilon'} \end{aligned} \tag{2.10}$$

With the information of the material properties, we can define the complex propagation constant (k).

$$k = \omega\sqrt{\mu(\epsilon' - j\epsilon'')} \tag{2.11}$$

$$jk = \alpha + \beta = j\omega\sqrt{\mu\epsilon'\left(1 - j\frac{\epsilon'}{\epsilon''}\right)} \tag{2.12}$$

Using the imaginary part of the propagation constant, we can now calculate the

propagation loss (α) inside the material with units Np per m.

$$\alpha = \omega \sqrt{\left(\frac{\mu\epsilon'}{2}\right)\left[\sqrt{1+\left(\frac{\epsilon'}{\epsilon''}\right)^2}\right] - 1} \tag{2.13}$$

Note the conversion from Nepers per m to dBm is:

$$\begin{aligned} 1\,\mathrm{Np} &= \frac{20}{\ln 10}\,\mathrm{dB} \\ &\approx 8.685559\,\mathrm{dB} \end{aligned} \tag{2.14}$$

Table 2.3: Calculated transmission coefficient of various materials with constant thickness at 5mm

Material Types	**Transmission Coefficients**
Air	0.98
Glass	0.95
Plexiglass	0.85
Water	0.20
Paper	0.86
Wood	0.60

The power loss due to reflections based on a multi-layer system, in this case, an air-material-air system (three layer system).
Using the reflection and transmission coefficients:

$$R = \frac{(1-Z_{12})(1+Z_{23}) + (1+Z_{12})(1-Z_{23})e^{-2\gamma_2 d}}{(1+Z_{12})(1+Z_{23}) + (1-Z_{12})(1-Z_{23})e^{-2\gamma_2 d}} \tag{2.15}$$

$$T = \frac{4}{(1-Z_{12})(1-Z_{23})e^{-\gamma_2 d} + (1+Z_{12})(1+Z_{23})e^{\gamma_2 d}} \tag{2.16}$$

where

$$Z_{ij} = \frac{\mu_i \gamma_j}{\mu_j \gamma_i}, \quad i,j = 1,2,3\ldots$$

and

$$\gamma_k = \pm\sqrt{j\omega\mu_k(\sigma_k + j\omega\epsilon_k)}$$

$Z_{i,j}$ each represents the impedance of the air-medium-air materials.

Chapter 3 Methodology and Experimental Setup

This chapter will discuss the equipment and setup used in carrying out the experimental investigation of the research questions. Based on these understandings, we have selected a specific combination of hardware to be used in our studies. The construction and justification for the testing form sample are also explained in this section according to the defined factors. The analysis method and software used will be briefly elaborated. We will also discuss the simulation software that was used in designing the antenna.

3.1 Governing Factors

Previous work in the laboratory has investigated and selected the key factors that affect the readability of a single RFID tag. [17, 23, 18] Table 3.1 and Figure 3.2 show the key factors that were investigated and their description.

Table 3.1: Governing factors on the readability of a RFID tag

Factors	**Descriptions**
Air gap	Distance between face of antenna and sample form
Tag space	Relative distance between each tag
Tag orientation	Angle varied about the axis normal to tag face.
Power level	Power emitted by antenna which can be set in the radio software
Tags number	Number of tags on a sample form

3.2 Sample Forms

We pre-programmed the tags with known IDs and known tag spacing, and then affixed them on a paper. As shown in the Figure 3.1, there are 5 uniquely programmed tags on the paper with the Target Tag surrounded by 4 similar tags. These testing samples with tags affixed in different combinations of tag spacing and tag type are considered a "Sample Form". Then, we wanted to reliably couple/read the target tag only using a single Antenna directly above it.

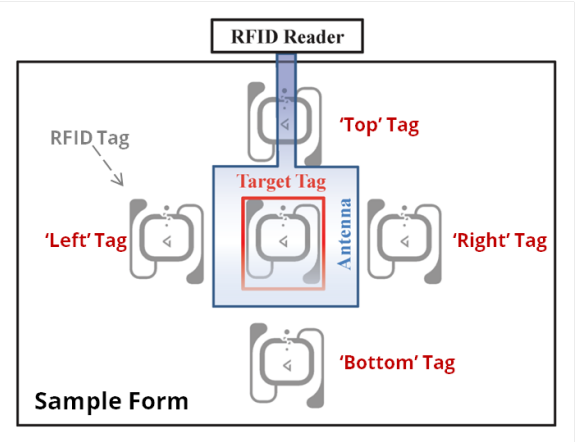

Figure 3.1: Sample form with 5 tags

3.3 Experimental Testing Platform

This testing platform, shown as Figure 3.2, was custom built by previous students for investigation of factors affecting the readability of a single UHF RFID tags. The materials selected in the experiment are mostly RF transparent so the material effects can be isolated. [14] Recently, the device was modified to improve the reliability of the system based on the literature review about material effects.

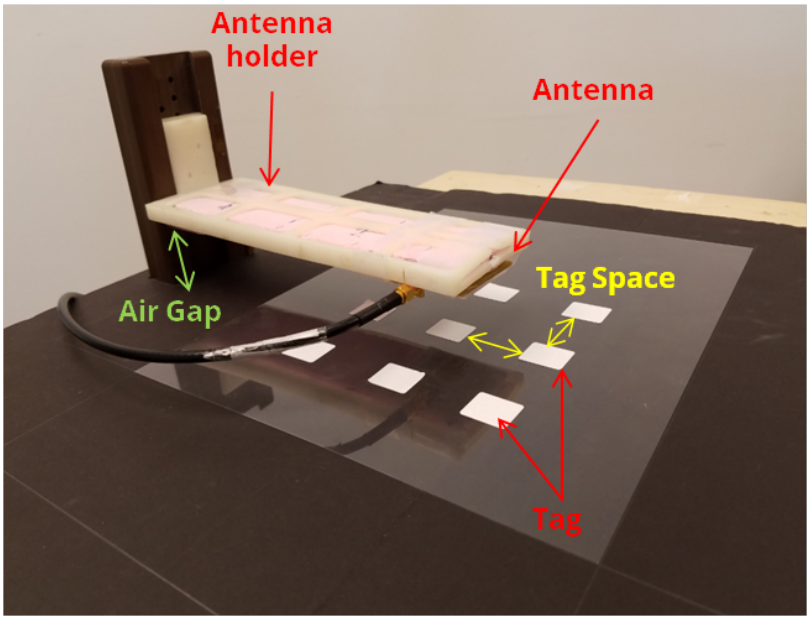

Figure 3.2: Testing Fixture Setup

Figure 3.2 shows the key components of our equipment (in red) and how a static read test is typically carried out. We positioned the sample form on a black foam

board, and we switched the form after a test run is completed. The Antenna with coax cable feed was held and positioned directly above the target tag, and its height can be freely adjusted by raising/lowering the holder. The design of the new testing platform will be discussed in detail in Chapter 5.

3.4 Equipments and Tags used

In this section, we discuss the materials selected to be tested and some of the equipment that was necessary to carry out the testing. For most of the investigations performed in the fourth chapter, we carried out the experiments in our own laboratory, Ralph G Anderson Building room 210b at the university. Due to the nature of our experimental device and settings, we do not require an anechoic environment free from external EM interference. In most setup, the power radiating from the antenna was well within the government regulation and the operating distance was usually less than a quarter-wavelength.

However, for testing that is sensitive to RF interference, like the investigations in the fifth and sixth chapters, we utilized the RF anechoic chamber at Lexmark Engineering Building in Lexington, Kentucky. It is a $5m$ chamber that is fully covered in pyramidal Radiation Absorbent Material.

Reader

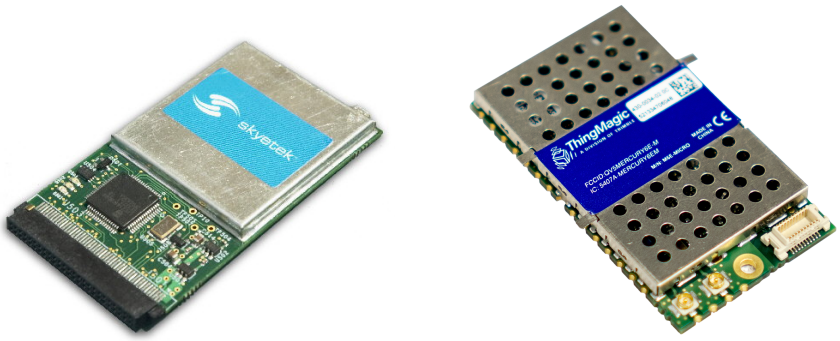

(a) Skyetek™ SkyeModule M9 (b) ThingMagic™ Micro M6E

Figure 3.3: Radios selected for experiments

In order to transmit and interpret the RF signal in the UHF band, we first used the Skyetek™ SkyeModule M9 radio, shown in Figure 3.3a, in our setup to complete the experimental tests. The preliminary investigation of multi-up was completed based on this radio setup to maintain consistency over previous single tag research. Using the same radio setup, it allowed us to compare some of the single tag read results versus tag read results in a multiple tags environment.

After the fifth chapter, we upgraded to a more recent radio to accommodate our new experimental testing platform, using the ThingMagic™ Micro M6E, shown as Figure 3.3b. It is a low-energy 2-port UHF RFID Module. This radio was selected because of its performance and its versatility. It has a high power level sensitivity of 0.5 dBm above +15 dBm, so we were able to accurately adjust the power transmitted and maintain a more consistent test performance compared to the previous radio.

This radio also has the ability to switch between several frequency regulatory specifications (from 860 mHz to 960 mHz) or disable frequency hopping. This enabled us to test a lower end of the UHF band if necessary. Besides, this reader has the capability to display the Received Signal Strength Indicator and phase angle. This was particularly useful because it provided a certain degree of observations to our measurements.

For the purpose of this experiment, frequency hopping was not disabled to imitate a real-world RFID operation. We wrote a C# visual studio program in order to select the parameters and to output the results in a way that can be easily interpreted. This will be further explained in Chapter 5. For each material, 5 different power level were used in the experiment. The list of power levels (and wattage conversion) used are listed in Table 3.2.

Table 3.2: Proposed power level for the transmitting antenna

Power Level	
(dBm)	(≈ Watt)
27.0	0.50
22.8	0.19
18.5	0.07
14.2	0.03
10.0	0.01

Antenna

Two different type of antennas were selected for use in the experiments in the fifth chapter. They were the custom Skyetek™ Single Loop Antenna and custom Lexmark Single Loop Antenna. The one shown in Figure 3.4a is a 7.5 inch circularly polarized micro-strip antenna. This antenna was selected as the main transmitting antenna. In general, they have a figure '8' radiation pattern which was slightly directional. They were setup horizontally on a foam holder above the tags media with the beaming direction facing down, shown as the grey box in Figure 3.4a. The new antenna design inspired by out test results will be explained in detail in Chapter 6.

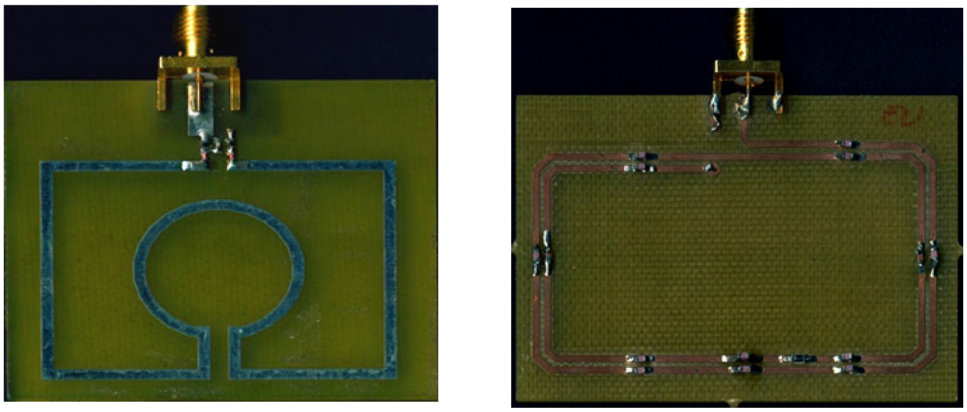

(a) Skyetek™ Loop Antenna (b) Lexmark Loop Antenna

Figure 3.4: UHF loop antennas

Tags

Three passive UHF RFID tags were selected. They were UHF RFID Inlays from two different manufacturers. Alien Technology ALN-9714 "Bio" and Alien Technology ALN-9629 "Square" were selected due to their size and consistent performance of the tag antenna. Although they have relatively smaller read range compare to other bigger size RFID tags, we selected them because of their symmetrical and square shape. [15] SMARTRAC DogBone was the tag that was selected and simulated in the later chapter. We preferred this tag because it was shown to exhibit relatively high readability compared to other tags. [23]

(a) SMARTRAC DogBone (b) Alien Technology Bio (c) Alien Technology Square

Figure 3.5: Three of the main tags used in the experiment. Tags (b) and (c) are suitable for near field application but with limited read range. (Not to scale)

3.5 Softwares

The results were collected and formatted to be analyzed via ANOVA test. ANOVA was chosen to show the statistical analysis of the significant difference between different factors. Minitab version 16 was used to carried out this particular analysis. In

the future, we also want to evaluate the performance difference between placing the testing device in the anechoic chamber and in the real-world environment.

In chapter 6, to validate our proposed antenna design, a finite element method solver for electromagnetic structures, ANSYS™ HFSS, was used to simulate the antenna design. Some in-depth comparisons were made between the experimental data to the simulated data in the software. Prior to the simulation, classes and seminar were taken to learn the operating language and functionality of the simulating software.

Chapter 4 Experimental Investigation on Tags Configuration Affecting the Programming of Multiple Tags

In this chapter, we will investigate how tag placement affects the readability of the target tag. To better understand the motivation of this chapter, we will use Figure 4.1 below to explain. The figure shows a stream of closely arranged tagged boxes on the conveyor belt, each of them pre-programmed with different shipping information. When they pass under the antennas, each of the boxes directly under each antenna was identified and sorted accordingly to identify the proper destination for each box.

Hence, we were interested in investigating the factors that affect the detection and activation of the neighboring tagged boxes the most.

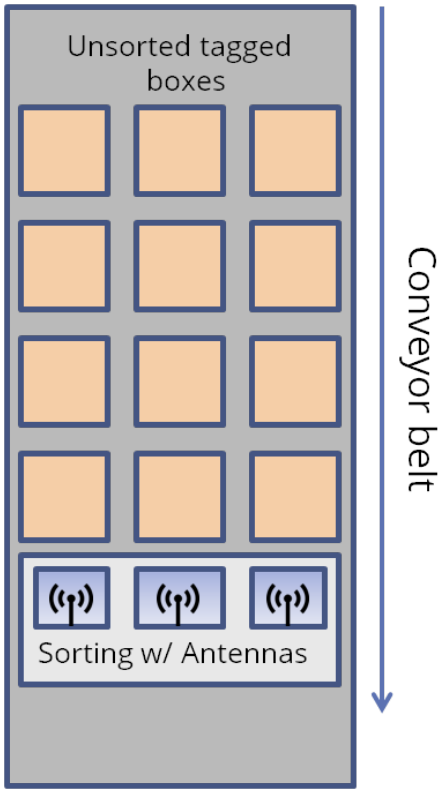

Figure 4.1: Purpose of the thesis

The major problem occurred when a group of tags was unintentionally activated at the same time. In those instances, the reader was not able to identify the data of the tag correctly when more than one tag occupied the same communication channel, a phenomena known as tag-to-tag collision/interference. The phenomena is illustrated

in Figure 4.2. In this scenario, there was also reader-to-reader collision but that was not our main focus.

There are a few ways to reduce these interferences; for example, the anti collision algorithms, localization of each tag and a better antenna design. Current localization techniques still have a relatively large margin of error to be used reliably in our application. But in this chapter, we are looking to accomplish it by physically varying how the tags are placed apart from each other.

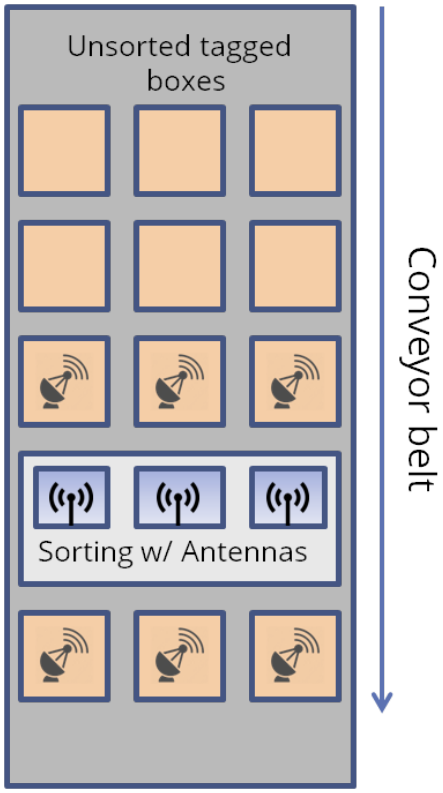

Figure 4.2: Challenges of the scenario

Test Setup

To replicate the desired scenario, we pre-programmed the tags with known IDs and known tag spacing, and then affixed them on a paper. As shown in Figure 3.1, there were 5 uniquely programmed tags on the paper with the Target Tag surrounded by 4 similar tags. These papers are the "sample forms" explained in Chapter 3.3. Then, we wanted to reliably couple/read the target tag only using a single Antenna directly above it. Figure 3.2 shows an example of how a test is conducted.

Table 4.1: Experimental Factors and Levels

Tag Type	Power Level (dBm)	Tag Space (mm)	Tag Orientation
Alien "Bio"	10.0	50	0°
Alien "Square"	14.2	40	180° [1]
	18.5	30	270° [2]
	22.8	20 [2]	
	27.0		

[1] Tested with Alien "Square" only, [2] Tested with Alien "Bio" only.

4.1 Experimental Factors

In this section, we describe the governing factors that affect the target read rate (readability) for both the tags. Air gap is the distance between face of antenna and sample form. Tag Space is the distance between two tag centers, which is varied from 20mm to 50mm. Shown in Figure 4.3, two best tag orientations are chosen for both the tags tested. Power level is the power emitted by antenna (which is set in the radio software). Refer to Table 4.1 for more detail.

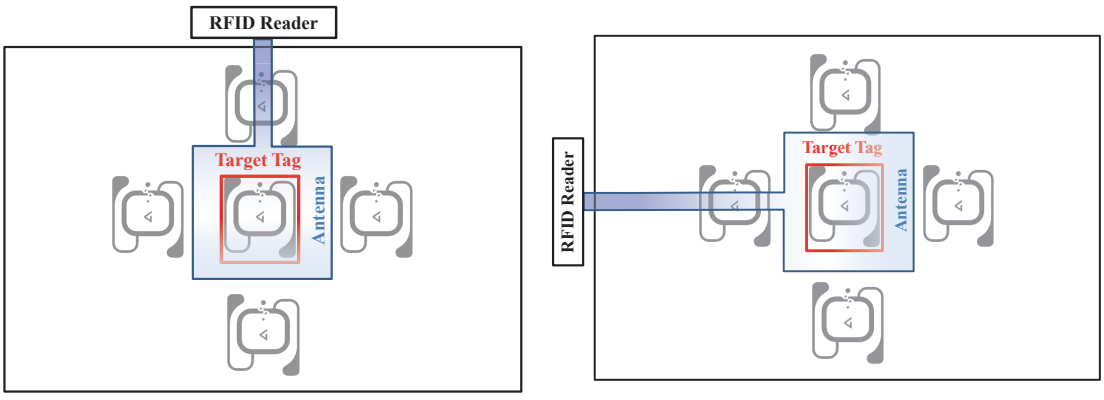

(a) Tags oriented at 0° (b) Tags oriented at 270°

Figure 4.3: Example of Alien "Bio" Tag Orientations

According to the general conclusion proposed in [9, 22], and confirmed in [23, 18, 17], tag read rate in the near-field region can also be significantly impacted by a reader's power level. Since the power level could be equally or more significant as the

tag spacing, the five different power levels presented in Table 4.1 were investigated.

The number of tags was held constant at 5 and the tag pattern was also the same for all factor levels, as shown in Figure 4.4. Four non-target tags were arranged with the same distance to the target tag center along one axis, providing, a similar opportunity for non-targeted tags to be detected for the chosen factor levels presented in Table 4.1.

The tag spacing levels were defined as the distance from the IC center of a target tag to the IC center of an adjacent tag along one axis, as illustrated in Figure 4.4. It was a unique variable in the multiple tags experiment compared to the single tag investigations presented in [23, 18, 17]. Interference to the target-tag from proximity non-targeted tags was expected to vary significantly with tag spacing.

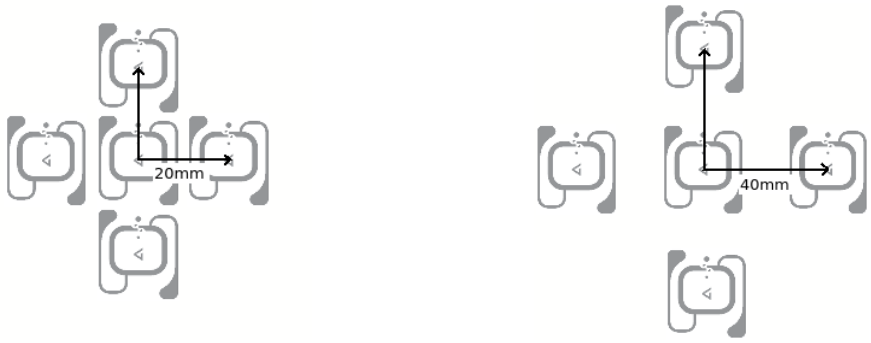

(a) Alien "Bio" 20mm (b) Alien "Bio" 40mm

Figure 4.4: Tag Space Used in the Experiments

4.2 Result and Analysis

For this study, the desired criteria include:

1. No non-targeted tags being detected
2. A sufficiently high read success rate of the target tag

Read success rate is defined as the number of positive reads in 100 successive attempts to read tag data. Table 4.1 presents the specific factor levels (5 different power levels, 4 different tag spaces and 2 different tag orientations) investigated in this study and Figure 4.6 shows typical results for the Alien "Bio" tag compared to a single tag. The target tag readability of Alien "Bio" overall was 28.0% for a target tag in a field of five tags when no non-targeted tags were detected. Compared to a maximum single tag read success rate of 63.4% (Figure 4.5) for the same conditions,

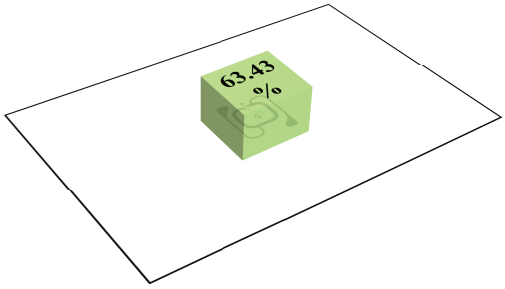

Figure 4.5: Alien "Bio" Single Tag Readability

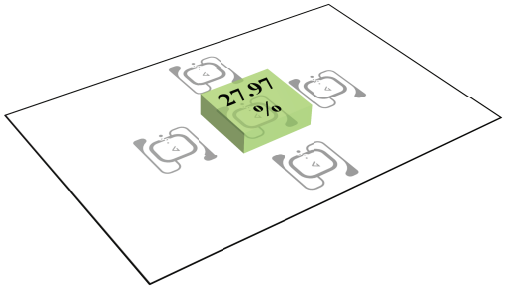

Figure 4.6: Alien "Bio" Multi Tag Readability

this resulting read success rate (with no non-targeted tags detected) was significantly lower.

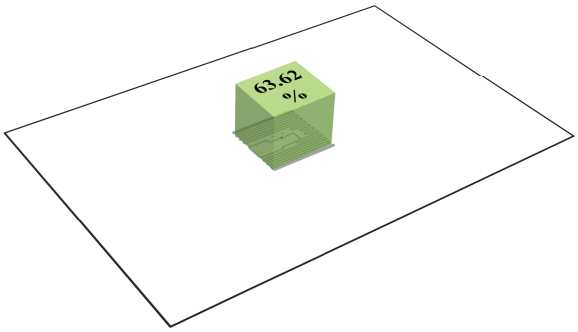

Figure 4.7: Alien "Square" Single Tag Readability

Similarly, results on the Alien "Square" tag are illustrated in Figures 4.7 and 4.8. This tag was examined for the 5 power levels, 3 tag spaces and 2 tag orientations listed in Table 4.1. For this tag, a small number of non-targeted tags were still detected at the positions shown for a read success rate of 8.6% (a drop from 63.6% of the read success rate of a single Alien "Square" tag for the same conditions).

To better understand the effect of the design factors on the read-success rate for multi-tags, a full factorial design was employed. The design was run at a single air gap for each of the two tags (5 mm for the Alien "Bio" and 10 mm for the Alien "Square"); the design factors studied were tag orientation, tag spacing and RFID reader power level. The specific mixed levels studied are given in Table 4.1 and three

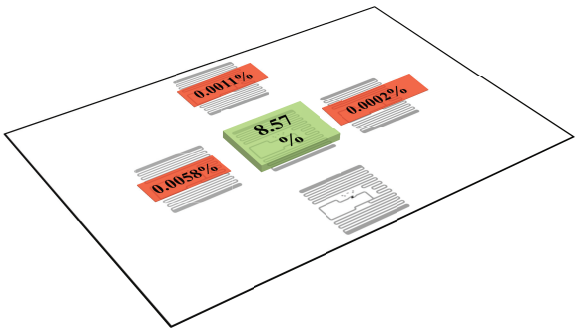

Figure 4.8: Alien "Square" Multi Tag Readability

replicates were obtained for each configuration [2]. The effect of factors and their interaction are shown in Tables 4.2 and 4.3.

Table 4.2: Table of Anova for Alien "Bio"

Source	F-Value	F-crit	P-Value
Main effects			0.000
Power Level	311.43	2.48588	0.000
Tag Space	78.22	2.71879	0.000
Tag Orientation	0.78	3.96035	0.381
2-Way Interactions			0.000
Power Level*Tag Space	10.11	1.87526	0.000
Power Level*Tag Orientation	2.99	2.48588	0.024
Tag Space*Tag Orientation	58.13	2.71879	0.000

Table 4.3: Table of Anova for Alien "Square"

Source	F-Value	F-crit	P-Value
Main effects			0.000
Power Level	180.1	2.52522	0.000
Tag Space	296.43	3.15041	0.000
Tag Orientation	1.96	4.00119	0.166
2-Way Interactions			0.000
Power Level*Tag Space	68.66	2.09697	0.000
Power Level*Tag Orientation	2.1	2.52522	0.092
Tag Space*Tag Orientation	3.56	3.15041	0.035

For this setup, the level of significance was determined at $\alpha = 0.05$. Tag orientation was found not to be statistically significant at the examined levels of 0 and 180 degrees (tag main axis aligned parallel with the antenna), as expected. This is also

verified in Figure 4.9. However, the power level and tag spacing were both found to be significant at the levels investigated, as were the effect interactions power level* tag space and tag space*tag orientation. The effect interactions may be more significant, in part, due to the large effect of power level for the Alien "Bio" and tag spacing for the Alien "Square" tag, respectively.

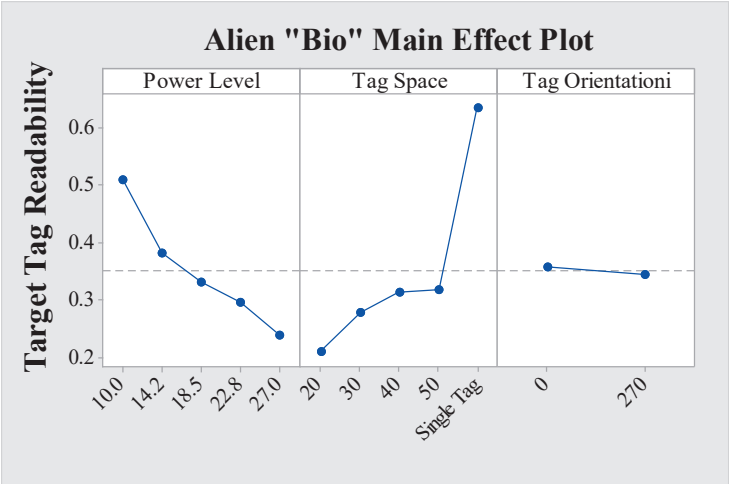

(a)

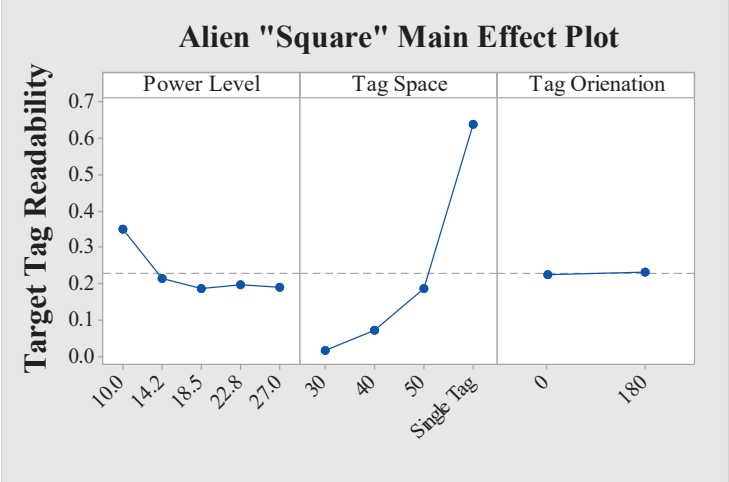

(b)

Figure 4.9: Main Effect Plots

As illustrated in Figure 4.9, the target tag readability decreases as the power level increases (as the magnetic field encompasses multiple tags). Moreover, the target tag readability increases as tag space increases (i.e., as the target tag in the multiple-tag environment approaches the conditions of a single tag). Thus, the target tag is best detected at relatively low power level and larger tag spacing.

As seen in Figure 4.9a, the power level has an approximately linear effect on the

tag read success rate for the Alien "Bio" tag. However, the effect of tag spacing on the read success rate is essentially flat for tag spacing greater than 40 mm. For the Alien "Square" tag, the effect of power level is essentially flat for a power level above 18.5 dBm, while the tag spacing has an approximately linear effect on tag read success for tag spacing between 30 and 50 mm.

4.3 Chapter Conclusion

Based on the design factors of tag orientation, tag space and power level, we analyzed the results to find the effect of these factors on the tag read success rate in a multiple tags environment. The results have shown that, tag orientation is not significant at the levels investigated for both the tags. However, the power level and tag spacing both have a significant effect on the read success rate. According to the models assumed for the full factorial designs, the target Alien "Bio" tag is best detected (in a field of five tags) at a very low power level (14.2dBm or less) and a tag spacing of at least 30 mm. The target Alien "Square" tag is best detected (in a field of five tags) at a low power level (18.5 dBm or less) and a tag spacing of 50 mm.

Hence, once we are able to read the target tag reliably, we are able to read all the other tags on the sample form based on the factor levels established. By moving the antenna to each of the location of the tags, we are able to maintain the reliability and consistency over the course of read operation of the sample form.

Chapter 5 Design of a Multiple Tags Testing Platform

This chapter describes the design, material selection and prototyping of the new testing platform. It will cover the selection of components that are used to move the antenna and the integration of the reader into the testing device. Some preliminary feasibility tests are also discussed.

5.1 Purpose

Continuing from the previous chapter, we designed a new testing platform to read all other tags on the sample form. Using the levels we established in Chapter 4, we wanted to verify if the performance of a single target tag read can be translated to other non-targeted tags. Figure 5.1 shows the proposed idea to move the antenna to the next tag, then read it. This process was repeated until all the tags in the sample form had been read. The idea was, under the same conditions established in Chapter 4, we could read other non targeted tags by repositioning the reader's antenna to each of the locations.

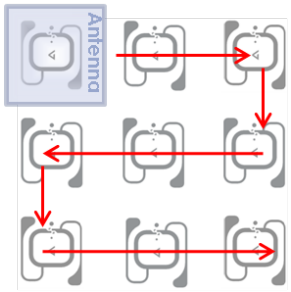

Figure 5.1: Movement of the antenna

Limited to only a static read operation, our current experimental device did not have the capability to move in two directions to accommodate this type of testing. In addition to building a device that enabled multiple tags read functionality, we designed the new testing platform to also provide the capability for us to run more test configurations, as needed (i.e., modular design).

Proof of Concept

The initial proof of concept design explored the feasibility of a multi-tag testing platform using a Lego™ Mindstorms controller, as shown in the bottom of Figure

5.2. This conceptual device had the capability to feed a sample form and move the antenna to each of the tags on the sample form.

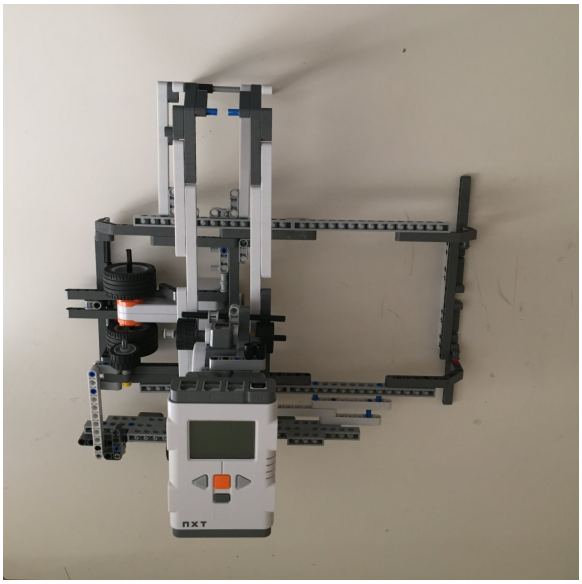

Figure 5.2: Proof of concept testing platform using Lego™

The device had two motors that moved a sample form based on the feedback from a color sensor. Building and programming using the Lego software were relatively simple, allowing us to rapidly test the feasibility of certain features that were desired in our prototype.

5.2 Design Criteria

Overall, the most important testing platform specification was minimal RF interference on the properties of the operating antenna. One of the most prominent factors affecting readability is material effects. In a near-field region, this affects the performance of read and write operations, producing undesirable results. Materials that are used to house the RFID tags and objects in nearby environments can impact the performance/readability of the tags from a distance.

This material effect can cause the adoption of RFID technology in certain environment difficult to be implemented. [14] RF waves are highly sensitive to metallic object and water-based liquids as they can alter the characteristics of the antennas. [24] We also reviewed literature of tags programming in an electronically cluttered area, in which a lot of metallic components are present.

Also, we wanted to be able to move the antenna to any points on the sample form for different combinations of tag spacing. Additionally, this array of tag locations should be to be easily modified when a new type of sample form is introduced.

Furthermore, we wanted this testing platform to be modular so additional type of testings can be accommodated and integrated into the device for future needs.

5.3 Hardware and Software

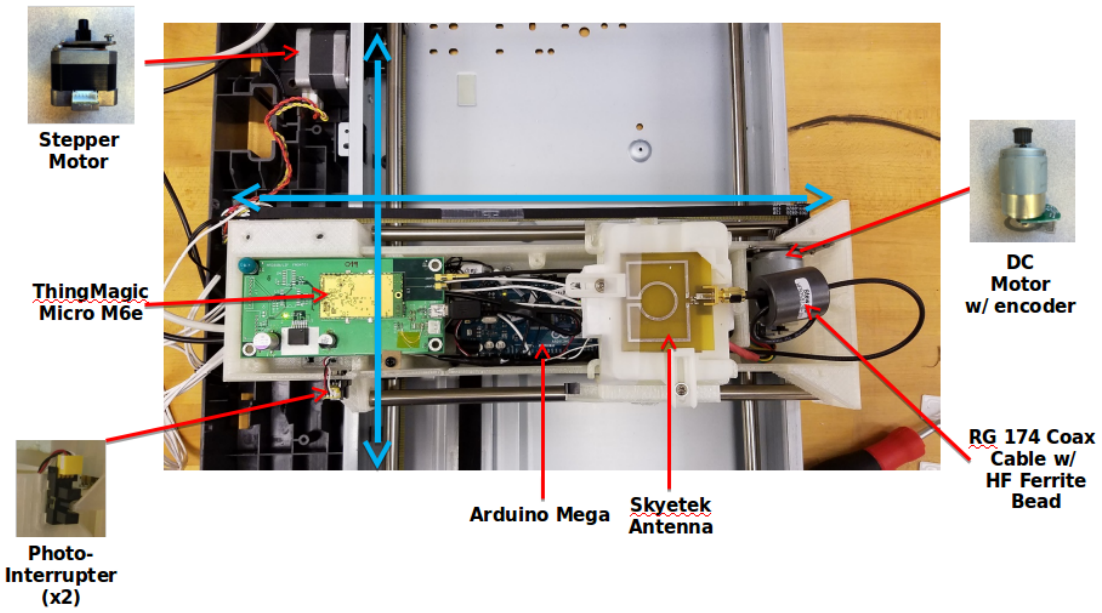

Figure 5.3: New testing platform with detailed labeling

Motion Control Components

In order to have 2 degrees of motion, we needed 2 motor units to move in each direction, as shown by the light blue arrows in Figure 5.3. The original scanner device platform already had a stepper motor and belt system built in. The use of stepper motor enables precise control of the motion; By calculating the steps, we were able to accurately track the position of our carriage. In our design setup, It was very important to have lightweight components on the carriage to reduce load on the stepper motor.

In order to enable the 2nd degree motion, we decided to use a lighter and smaller DC motor with a built in encoder to move and track. Shown in Figure 5.3, two photo-interrupters were used to inform and calibrate the carriage to a home position every time a test was completed. All these motors units and drivers were controlled using a single Arduino MEGA located in the middle.

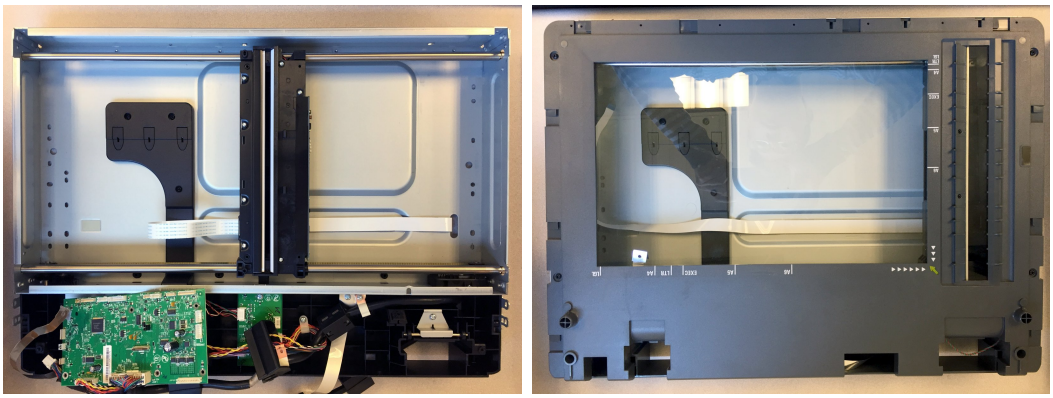

(a) (b)

Figure 5.4: Base platform of a scanner module

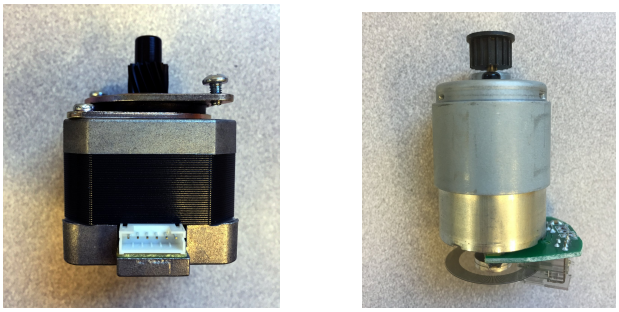

(a) (b)

Figure 5.5: Motor units used in moving the antenna

The only manual adjustment required in the testing device was the height of antenna holder. By raising or lowering the holder, we could adjust the separation between the antenna and tags just like out previous testing platform. This section sums up the selection and reasoning for the hardware and materials used.

Radio Control Setting

In order to program the tags, we used a ThingMagic™ Micro M6e reader placed in the left corner of carriage in Figure 5.3. It was connected to our existing Skyetek™ antenna with a 50ohm RG174 coaxial RF cable. Because the antenna was not perfectly matched to the radio source, some of the signals were reflected back to the coax cable, creating standing waves. These standing waves coupled with single shielded RG174 cable caused leakage along the cable line. Hence, 3 HF ferrite bead were wound around the cable to reduce undesirable activation of the RFID tags.

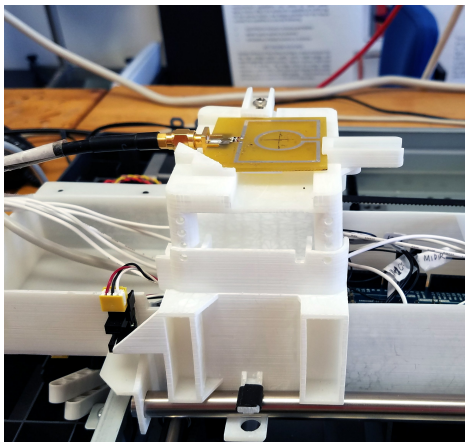

Figure 5.6: Manual adjustment of antenna holder for changing air gap

Software

In this section, we discuss the programming codes that are used to operate this new testing device and the preferences of using a certain programming language over the other. Figure 5.7 shows a simple flow diagram of the software structure.

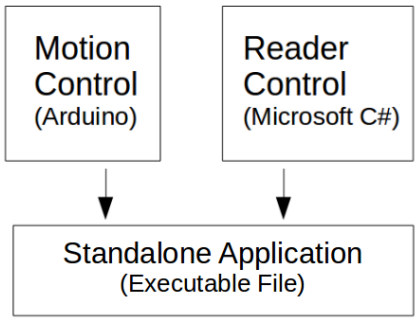

Figure 5.7: Programming languages used in each stages

For controlling the motion, the Arduino MEGA was an ideal microcontroller because it has large onboard memory to store the location arrays of tags of various sample forms and the script, so it made our testing device easily configurable when different sample forms were loaded. The communication to the reader was through a C♯ GUI (refer to Appendix) based on ThingMagic™ proprietary API. The configuration setting from the previous radio was replicated to ensure consistent results. Refer to the Arduino codes for details in the Appendix.

Lastly, we integrated these two programs to make a standalone executable program. Some preliminary testing showed that we were able to read all the tags on some of the sample forms. However, due to the inherently different setup from the

previous testing platform, the results had slightly different readability, but a consistent pattern. In the future, we keep the factors that are skewing the results between the two setups.

5.4 Prototyping

For the the first prototype, we used a Lexmark flatbed scanner module, shown in Figure 5.4, as a basis because it had some desirable features (like motor unit and a cover top) that could be incorporated into our testing platform. Illustrated as Figure 5.8, our first prototype carriage was printed using Stereolithography (SLA) method. The first prototype was fully functional and able to move the carriage with the antenna holder with ease.

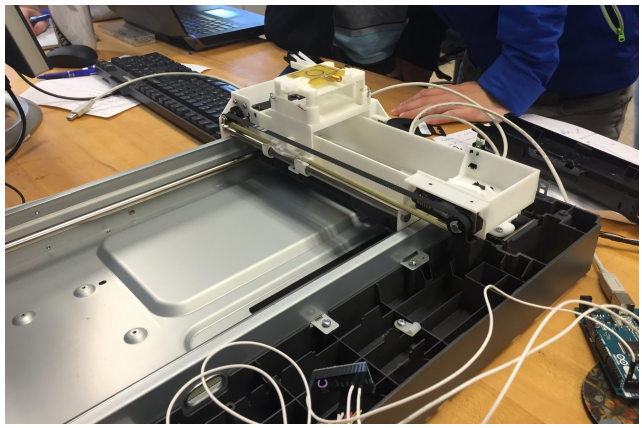

Figure 5.8: First generation of Multi-up testing platform

5.5 Problems and Improvements

Ultimately, there were some problems we encountered in designing the device, mechanically and electromagnetically.

Electromagnetic Interference

To ensure we have a good understanding on the degree of interference introduced, we conducted a study to investigate the effect of materials that affect the RF propagation through the material medium. Results are shown in Figure 5.9. In the experiment, we changed the supporting materials holding the sample form and then compared the relative effects on the readability. Please refer to Chapter 2 for more details on the literature. Some of the materials tested were wood, cardboard, polycarbonate and glass.

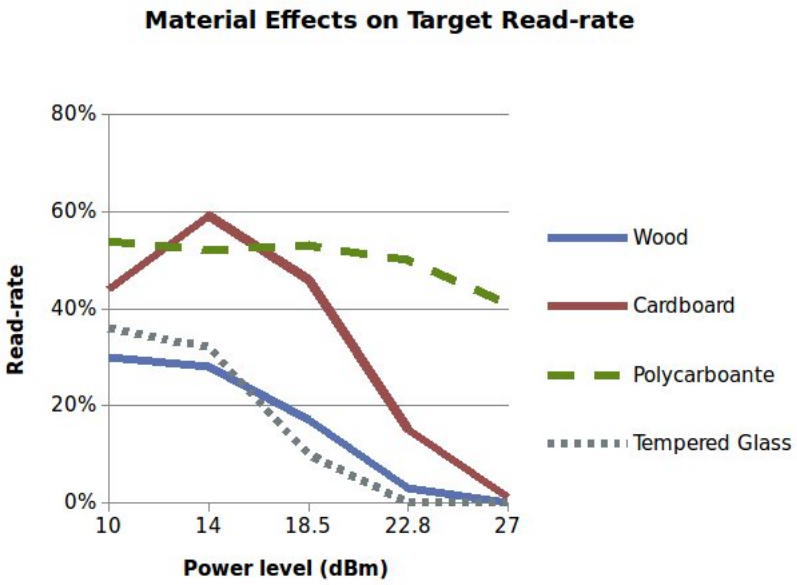

Figure 5.9: Materials effects on readability

According to our investigation and literature review, the scanner glass, which is made of tempered optical glass, caused a significant signal loss on the RF wave propagating through it. Typically, the scanner glass usually comes with an anti-glare coating composed partly of lead oxides which can explain the attenuation effects on the readability. So to ensure our results were not skewed significantly from the sample form holder, we replaced the glass with a solid sheet of Lexan polycarbonate of similar thickness.

Closely placed metals parts to the antenna tend to detune the antenna RF characteristic. So, similarly we replaced some of the metallic supports with a more RF friendly material, like polycarbonate or 3D printed PLA counterparts that met the mechanical requirement for structural integrity.

Mechanical Problems

After multiple test runs, we observed that the alignment of target tag and antenna position were off. It was discovered that the thin wall part of our carriage had experienced deformation and buckled, as shown in Figure 5.10a. SLA parts are weaker under stress, especially under belt tension from the belt pulley system. Initially, the buckling was temporarily fixed with tape holding both walls inward.

After a team design review, we changed in the model to strengthen the critical areas. More supporting struts were added and the wall of our carriage is thickened (shown as Figure 5.10b). Then, we reprinted the carriage and other parts using

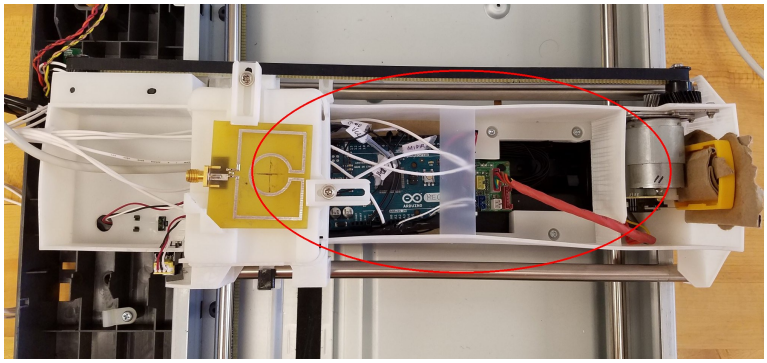

(a) Buckling of SLA wall over time due to belt tension

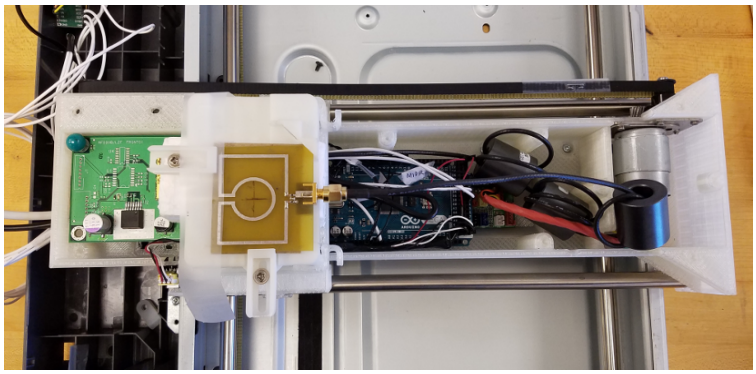

(b) PLA replacement carriage with a thicker wall

Figure 5.10: Carriage before and after replacement

a 3D printer with PolyLactic Acid (PLA) filament. As a result, our latest version (shown as Figure 5.11) was more rigid and stable with openings at places which required cable routing.

5.6 Chapter Conclusion

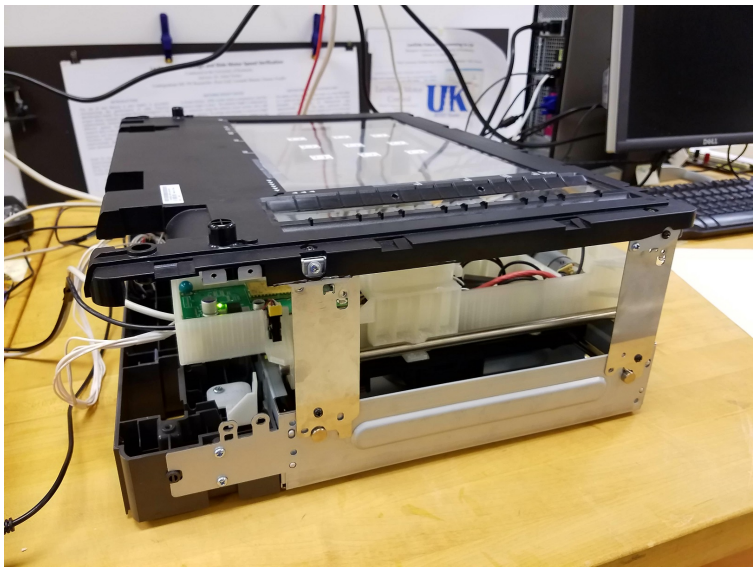

Figure 5.11: Latest generation of multi-tag testing platform

We have successfully built a new testing device that helps us to read multiple tags on a sample form based on the conditions established in the previous chapters. The transformation to the new testing platform also provides the capability for us to run additional test configurations, as needed. Based on our material studies, we have modified the testing device to be more RF friendly for reliable performance. After the optimal factor levels (which also satisfy the criteria) for reliable read operation are established, we can ensure our programming operation is similarly reliable.

Chapter 6 Design and Simulation of a Loop Antenna for Confined Electromagnetic Field Distribution

This chapter focuses on the specific antenna design for the multiple-tag application. Through previous experiments and analysis, antenna type has been discovered to be a big factor in our readability. However, an antenna design by nature is difficult to optimize and it is highly specialized. Hence, the antenna was the last factor to study after exploring all other available solutions, like changing tag type, modifying the tag layout, etc.

In this chapter, we discuss the criteria for the new antenna design and the reason why a certain type of antenna is preferred. This chapter will present some of the preliminary modeling and simulation of the new loop antenna (designated as Merida) along with the fabrication process.

6.1 Purpose and Criteria

Over the years, we have programmed a single RFID tag using a few different type of antennas. For a single tag environment, the characteristic of antenna was not as significant as other governing factors because we did not have to worry about accidentally activating other surrounding tags. Our aim was to have the highest single tag read rate. But for a multi-tag application, we discovered that the electromagnetic properties of the antenna could play a major role in a successful operation.

We began by searching for off-the-shelf components which matched our specific application and design criteria. However, most of the off-the-shelf antennas were physically large compared to our existing antennas. Most of them were intended for far field applications. So, we decided to look at designing our own antenna with the appropriate area and properties.

Shortcomings of Existing Antenna

If a RFID tag had a larger surface area compared to the antenna, we were not as concerned, as the antenna would not be overlapping other neighboring tags. By physically limiting the antenna to a smaller area, small size tags or narrower tag spacing could be used in our multi-tag operation. It was also important that this new antenna can be easily incorporated into the new testing platform.

Based on boundary Equation 2.2, the reactive near field boundary for UHF is

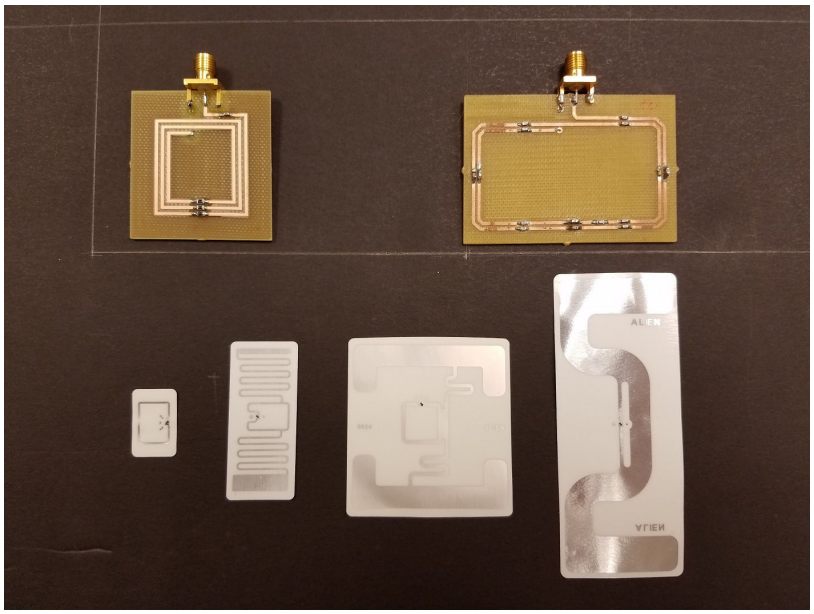

Figure 6.1: Comparison of antenna size and UHF tag size

calculated to be around 52mm. Most of our read operations were well within this boundary, so we aimed to design a UHF near field antenna which operated on magnetic induction. Since antenna design involves trial and error, we wanted to ensure we could rapidly and inexpensively develop some prototypes to validate our simulation model.

Literature Review

From some of the literature, there were a few possible low-profile antennas to be considered. First, we studied a printed Yagi Uda antenna. Due to the nature of UHF wavelength, the printed board would be relatively large, so the potential for activating more tags would increase. [31] The second antenna we looked at was a patch type antenna which has reasonably good performance in the far field region if it is used as a directional antenna. However, it was still relatively large compared to our existing antennas. [5, 3, 12]

Lastly, loop antennas usually have a strong magnetic field in the near field region. [22, 26, 10] They are usually used as receiving antennas because of the poor radiation resistance. For our application, we were not overly concerned with these limitations as we did not intend to use the antenna in a far field application. In general, a loop with diagonal dimension smaller than 1/10th of wavelength can be classified as an electrically small antenna. [4]

Simulation and Modeling

All simulations were completed using ANSYS™ HFSS (courtesy of Lexmark Inc). The frequency was swept using the "Fast" method to carry out the parametric sweep of the design variables. Once the resonant frequency was reached, the sweeping method was then changed to "Discrete" for more accuracy.

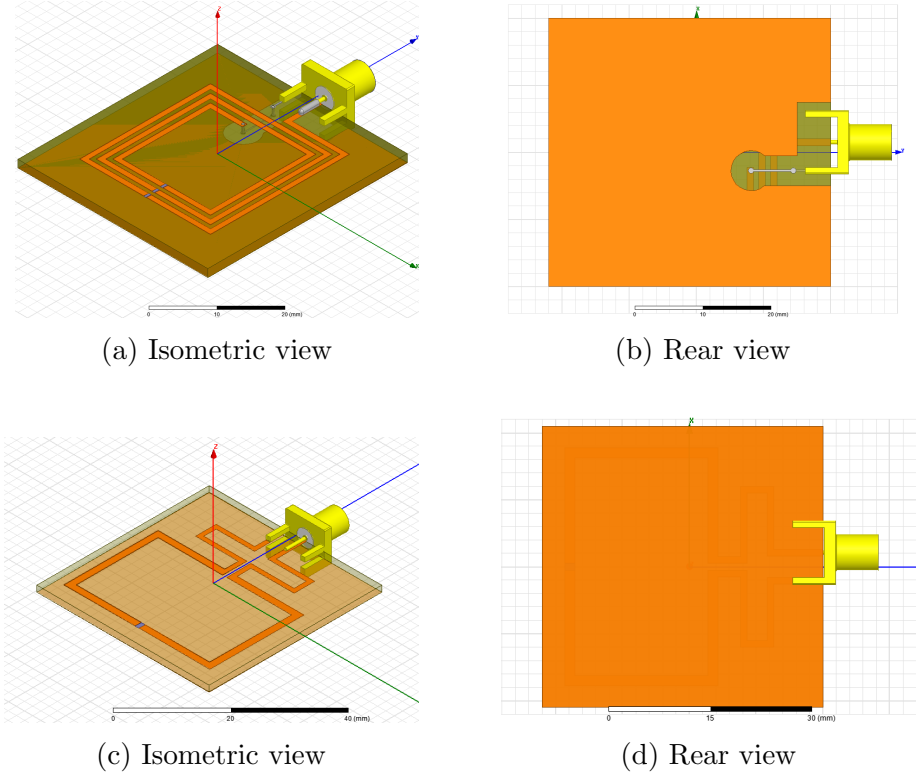

(a) Isometric view

(b) Rear view

(c) Isometric view

(d) Rear view

Figure 6.2: 3D Model of Merida v1.0 (a, b) & Merida v2.0 (c, d)

There were a few 3D parts to be modeled in HFSS: previous antennas for comparison, Dogbone RFID tags, SMA end launch connector, and a new antenna, shown in Figures 6.2. Version 2.0 was improved (and calibrated) based on version 1.0 after we obtained the true dimensions of the antenna (e.g substrate thickness and copper trace thickness) following the milling process. In addition, a simulation error was also discovered after the fabrication of Merida v1.0. Hence, the antenna was redesigned, verified and then re-fabricated.

Both versions of the antenna were designed to resonate at 915MHz with a return loss of at least -10 dB. They were designed to have physical dimension of $43mm \times 43mm \times 1.51mm$. Using the parametric function in HFSS, the width and dimension of the copper trace, which determine the inductance and capacitance of the circuit, were varied individually. Essentially, a RLC circuit was tuned to resonant at the UHF

band. A copper shield was added to the back of the antenna so that the coupling can only occur above the top of the loop.

6.2 Result and Analysis

Magnetic Field Performance Simulation

The most important result for our near field antenna design was the magnetic field distribution around the antenna. It determines the area where a tag is more likely to be activated and powered. So, 3 plane cuts were set at a distance of 20mm away from the top, bottom and side of the antenna. From Figure 6.3, the power level was set to be 15dBm. First, we observed that the concentrated magnetic field appears only on the top side of the antenna which was what we were aiming to achieve. The magnitude of magnetic field under the antenna is also lower than the magnitude on the top, reducing the probability of activating any non-targeted tags.

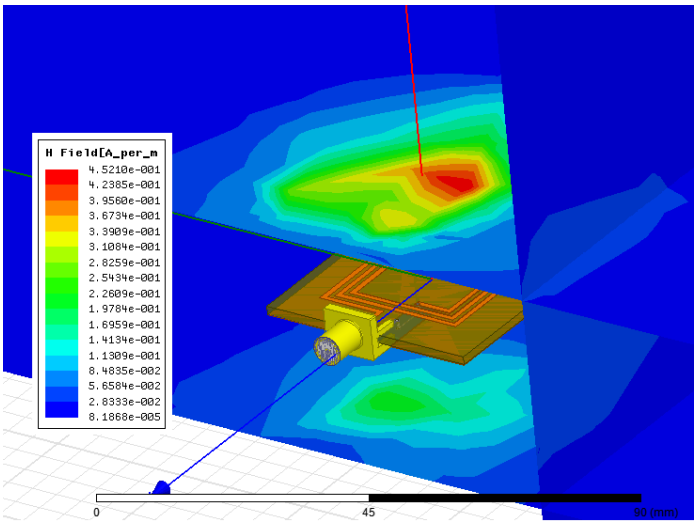

Figure 6.3: Magnetic field magnitude distribution of Merida v1.0

RFID Tags' Surface Current

To verify whether the antenna design has actually improved the target read performance while reducing the activation of non-targeted tags, we employed a method to compare the target tags and non-targeted tags relatively. Hence, to take advantage of the capability of HFSS, we simulated the surface current induced by the EM field on the dogbone tags emitted from the antenna below. By visually inspecting Figure 6.4, we compared the magnitude of surface current induced on two Smartrac "Dogbone" tags. To further verify the improvement, we could experimentally measure and compare the EM field emitted by the antenna in an anechoic chamber post-fabrication.

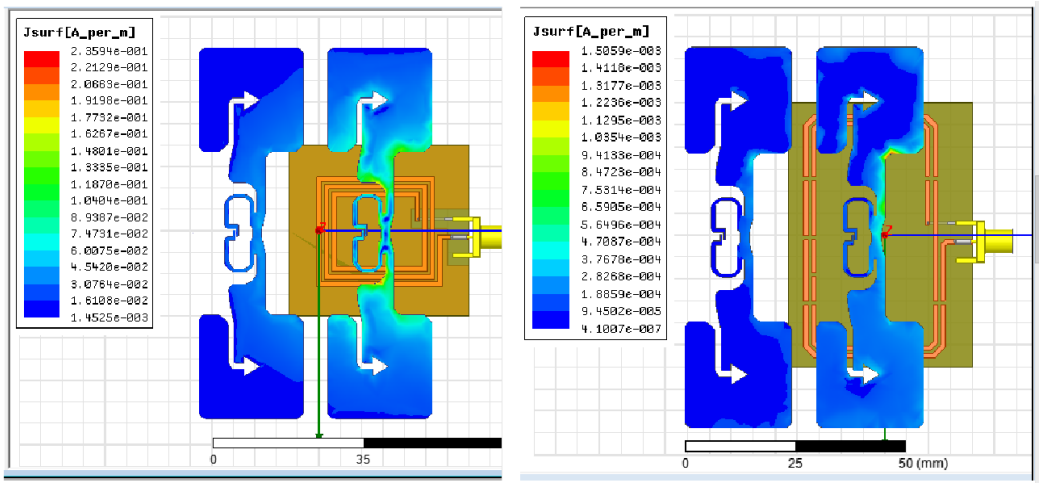

Figure 6.4: Comparison of Surface Current Induced between Lexmark Loop and Merida v1.0

$$\oint \vec{E} \cdot \vec{dl} \tag{6.1}$$

Using the formula for calculating voltage across a line (Formula 6.1), we calculated the voltage induced across the gap where the IC is located, as shown in Figure 6.5. A Comparison was made to the voltage generated by targeted tag and non-targeted tag, and then the results were compared between the old and new antenna.

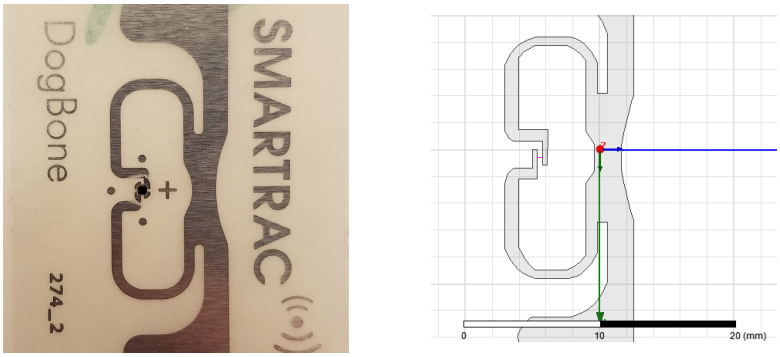

(a) (b)

Figure 6.5: Gap across the IC for voltage calculation

Fabrication and Comparison

After we confirmed that the simulation model was what we desired, we fabricated the first prototype antenna, Merida v1.0. Using Eagle, a PCB designer tool, we sketched

the copper trace and specified the drilling holes for the milling process. After milling out the unwanted copper, we soldered the copper SMA connector and resistors to the board. (Figure 6.6) The same fabrication process was repeated for Merida v2.0.

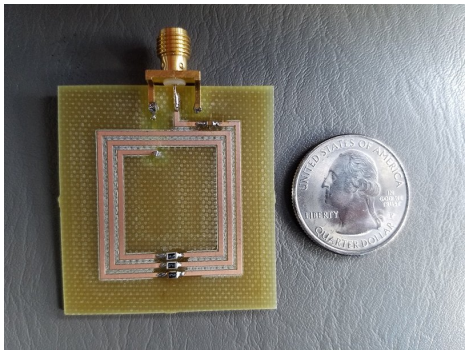

(a) Front view

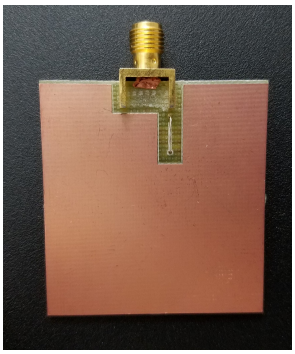

(b) Rear view

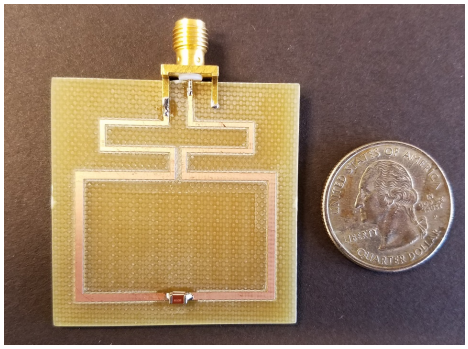

(c) Front view

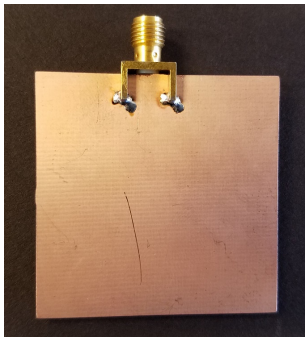

(d) Rear view

Figure 6.6: Fabricated Merida v1.0 (a, b) & Merida v2.0 (c, d)

Then, we measured the return loss of the fabricated antenna using a network analyzer (Agilent 4396B). The results for both versions of Merida is shown in Figure 6.7. The return loss measurement is important in order to understand the efficiency of an antenna in a particular frequency band.

Shown in Figure 6.7a, it appears that Merida v1.0 has a significantly different resonant frequency and value of return loss due to a simulation setting error. The measured resonance frequency of the lowest return loss lies at 1.26GHz compared to our simulated one at 915MHz. An error in simulation was discovered later and the corrected return loss curve was added to Figure 6.7a. However, there is still a difference of 100MHz (1.16Ghz vs 1.26Ghz) in resonant frequency post-correction of the simulation.

There are a few possible explanations for this result; we added a jumper cable to complete the loop because the milling machine had taken off too much copper at one

location. It was also possible that the larger size resistors might have a significant effect on the antenna characteristics. As the return loss at 915Mhz was only about -4dB, the antenna did not meet our design criteria.

The measurement for the 2nd version of Merida is shown in Figure 6.7b. The difference between simulated frequency and measurement is about 40 MHz, so it did not shift as much compared to the Merida v1.0. The measured return loss of the UHF band (902MHz - 928Mhz) is from -10.5dB to -13.5dB, which satisfies our design criteria. The antenna also showed a reasonably well performance in confining the magnetic field.

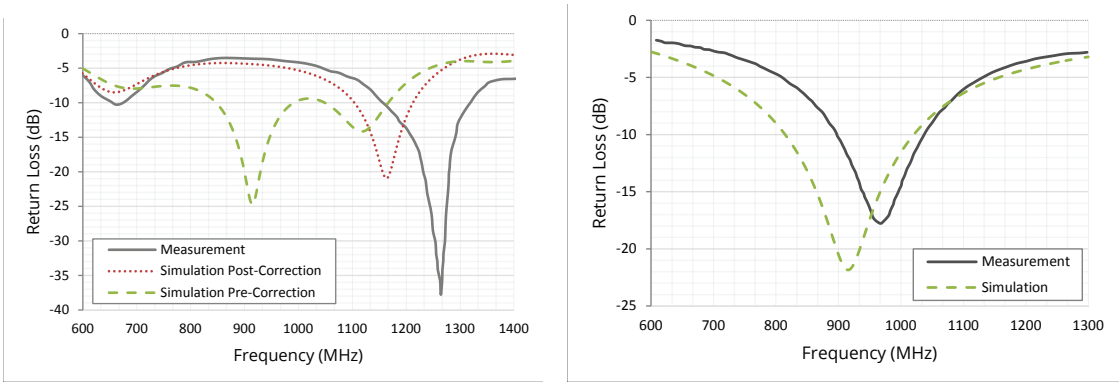

(a) Merida v1.0

(b) Merida v2.0

Figure 6.7: Comparison of Return Loss between Simulation and Measurement

6.3 Chapter Conclusion

The new antenna design, Merida v2.0, has shown desirable performance in targeting a single tag in a field of multiple tags. Compared to the old antennas, we are able to detect only the targeted tag more consistently under the same conditions established in Chapter 4.

However, the design of antenna is still a work in progress. For the coming step, we want to determine the difference in return loss plot between our simulated model and actual measurement. Then, we will go back to remodeling and simulation. Finally, a sensitivity test can be carried out to investigate the effects of trace dimensions in the antenna in order to tune the resonant frequency.

Chapter 7 Conclusion

We have addressed our research questions through Chapters 4, 5 and 6. We presented a model for reliably reading a target tag in the presence of other tags in a near field environment. As a result, we can begin investigating the efficacy of the new loop antenna along with the new testing platform.

The list below summarizes the conclusions and discoveries of the 3 chapters:

1. We investigated the factors affecting the optimum reading configuration for a multiple tags environment and discovered that tag spacing and power level are significant to the target tag readability.
2. We created a new testing platform to read every single tag on a sample form, with the capability and flexibility to run additional form configuration.
3. We redesigned our antenna to operate effectively in a near field system in order to further improve the target read performance of a tag.

Completion of this thesis has inspired some similar future work in which a more effective operation can be possibly achieved. As shown in Figure 7.1a, in the near future, we are looking to study the effect tag spacing patterns, like the picture shown on the left. Although we have concluded that the Alien "Bio" tag is not sensitive to tag orientation, there are several other tags which are sensitive to orientation. We can use this advantage to reduce the probability of activating the neighboring tags.

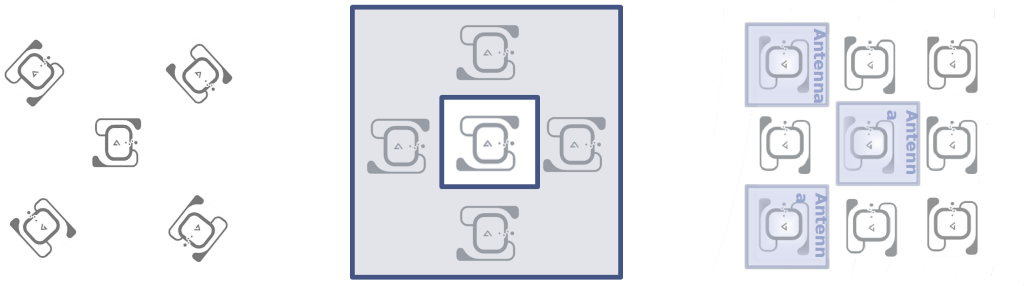

(a) (b) (c)

Figure 7.1: Proposed future work for further improving read operation

We also propose other mechanical means of isolating the tags from each other. For example, as shown in 7.1b, instead of avoiding metal near our sample form, we will

investigate the addition of a shield which will intentionally detune the surrounding tags' antennas. However, this will require a new antenna design which can work effectively with this shield. And lastly, once we are confident that the ideal parameters and a satisfactory antenna design have been identified and tested, we can scale the operation to increase the throughput rate.

List of Appendices

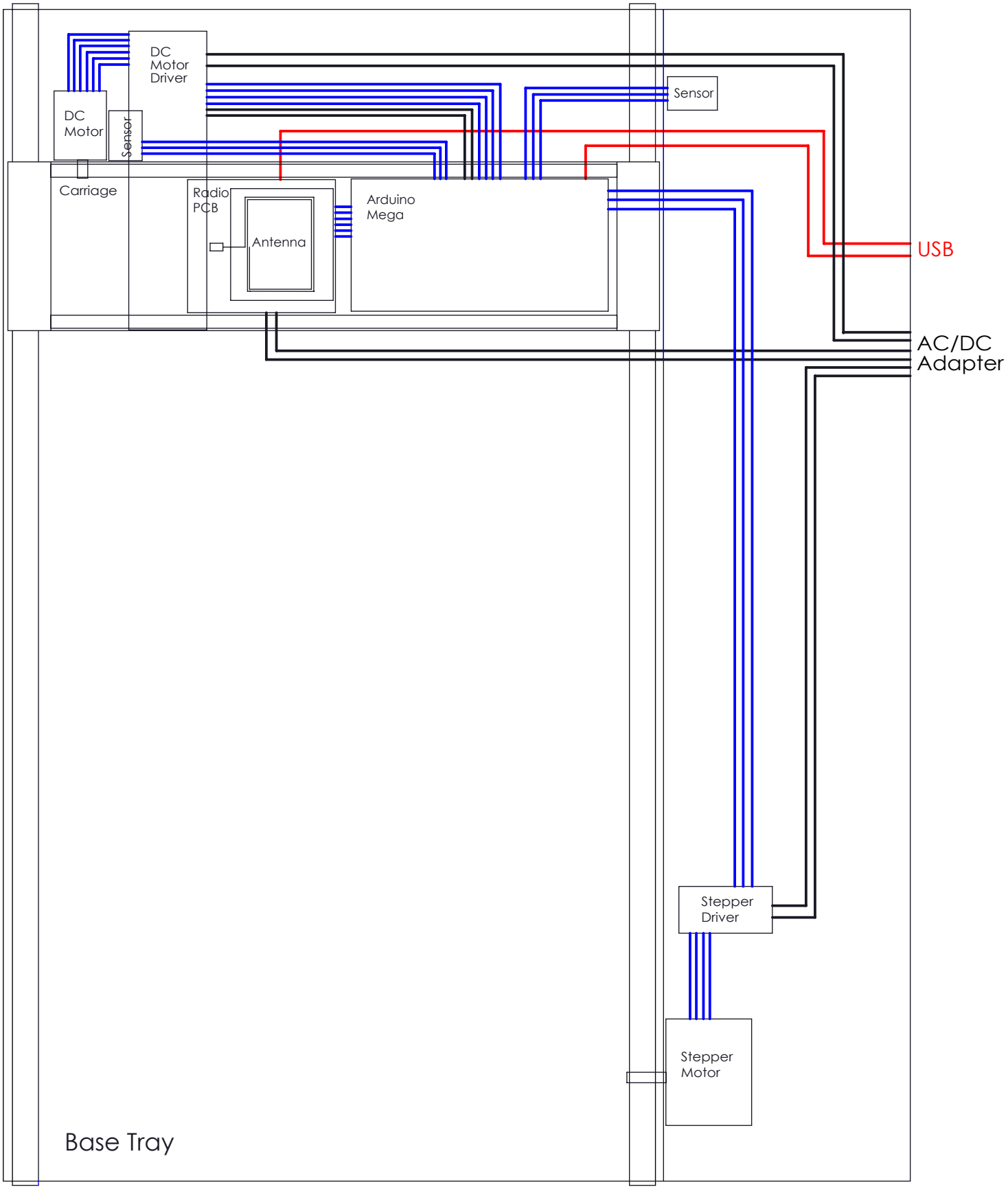

DIMENSIONS ARE IN MM
TOLERANCES: 0.0
FRACTIONAL ±
ANGULAR: MACH ± BEND ±
TWO PLACE DECIMAL ±
THREE PLACE DECIMAL ±

DO NOT SCALE DRAWING

DRAWN	Paul	9/8/2015
COMMENTS:		

UK RFID Multi-UP Circuit & Hardware

SIZE	DWG. NO.	REV.
A	DrawFinal	
SCALE:1:2	WEIGHT:	SHEET 1 OF 1

```
//Arduino Programming for 2 axis-motion control with sensors feedback.
//
//This code combines the two motor codes, DC with encoder and stepper motor, into a single
script. The //beginning section defines the pin-outs and wirings to the sensors and motors. An
array is used to //store the tags location of multiple sample forms.
//To add or change a sample form coordinates, modify the array and int length.
////////////////////////////////////////////////////////////////////////////////////////////
///////

#define s_step 37
#define s_dir 39
#define sleep_pin 36
#define encoderIn_y 53 // input pin for the interrupter
int detectState_y; // saves the status of the photointerrupter
int start_command; // asks for a command to start the stepper program
#define conv_y 0.0425 // mm per step
int case_number; // asks for a number to select the type of paper
#define wait_go 5
// the following is from the DC motor code
#define Dir 31 // Dir motor pin
#define PWM1 5 // PWM motor pin
#define encodPinA 2 // encoder A pin
#define encodPinB 3 // encoder B pin
#define LOOPTIME 100 // PID loop time
#define FORWARD 1 // direction of rotation
#define BACKWARD 2 // direction of rotation
#define encoderIn_x 52 // input pin for the interrupter
#define conv_x 0.037 // mm per step
int detectState_x = 0; // Variable for reading the encoder status
long count = 0; // rotation counter
long countInit;
long tickNumber = 0;
boolean run = false; // motor moves
int d; // distance the carrier moves in x direction

// this is the array which contains the x and y information of two paper types
int pos[16][9] = {
  {
    12 , 135 , 135 , 12 , 12 , 135 , 135 , 12
  } // dogbone
  , // X coordinates paper type 1 (9 tags, 50 mm)
  {
    105, 105, 174, 174 , 242, 242, 310 , 310
  }
  , // Y coordinates paper type 1 (9 tags, 50 mm) // dogbone
  {
    45 , 95 , 145 , 145 , 95 , 45 , 45 , 95 , 145
  }
  , // X coordinates paper type 2 (9 tags, 40 mm) // dogbone
  {
    185, 185, 185, 235 , 235, 235, 285 , 285, 285
  }
  , // Y coordinates paper type 2 (9 tags, 40 mm) // dogbone
  {
    77 , 27 , 77 , 127, 77
  }
  , // X coordinates paper type 3 (5 tags, 50 mm) // dogbone
  {
    112, 232 , 232, 232 , 352
  }
  , // Y coordinates paper type 3 (5 tags, 50 mm) // dogbone
  {
    77 , 37 , 77 , 117, 77
  }
  , // X coordinates paper type 4 (5 tags, 40 mm) // dogbone
  {
    122, 232 , 232, 232 , 342
```

```
  }
  , // Y coordinates paper type 4 (9 tags, 40 mm) // dogbone
  {
    27 , 77 , 127 , 127 , 77 , 27 , 27 , 77 , 127
  } // Alien square
  , // X coordinates paper type 5 (9 tags, 50 mm)
  {
    182, 182, 182, 232 , 232, 232, 282 , 282, 282
  }
  , // Y coordinates paper type 5 (9 tags, 50 mm) // Alien square
  {
    37 , 77 , 117 , 117 , 77 , 37 , 37 , 77 , 117
  }
  , // X coordinates paper type 6 (9 tags, 40 mm) // Alien square
  {
    192, 192, 192, 232 , 232, 232, 272 , 272, 272
  }
  , // Y coordinates paper type 6 (9 tags, 40 mm) // Alien square
  {
    77 , 27 , 77 , 127, 77
  }
  , // X coordinates paper type 7 (5 tags, 50 mm) // Alien square
  {
    182, 232 , 232, 232 , 282
  }
  , // Y coordinates paper type 7 (5 tags, 50 mm) // Alien square
  {
    77 , 37 , 77 , 117, 77
  }
  , // X coordinates paper type 8 (5 tags, 40 mm) // Alien square
  {
    192, 232 , 232, 232 , 272
  }
  // Y coordinates paper type 8 (5 tags, 40 mm) // Alien square
};

int lengths[8] = {8, 9, 5, 5, 9, 9, 5, 5}; //contains the amount of tags per paper (9 on the
first, 5 on the second)
int pos_x[9]; //array which receives the x position from the big pos[][] array
int pos_y[9]; //is used in stops();
int length = 0; // int which receives the amount of tags per paper
int num; // number which is used in stops();
int cur_x = 0; // saves the current x position
int cur_y = 0; // saves the current y position
int x;
int y;

// setup is only run once when the program is started; sends carrier to base
void setup()
{
  digitalWrite(s_step, LOW);
  pinMode(s_dir, OUTPUT);
  pinMode(s_step, OUTPUT);
  pinMode(encoderIn_x, INPUT);
  pinMode(encoderIn_y, INPUT);
  pinMode(Dir, OUTPUT);
  pinMode(PWM1, OUTPUT);
  pinMode(encodPinA, INPUT);
  pinMode(encodPinB, INPUT);
  digitalWrite(encodPinA, HIGH); // turn on pullup resistor
  digitalWrite(encodPinB, HIGH);
  attachInterrupt(1, rencoder, FALLING); // important for DC motor
  Serial.begin(9600); // selects the Serial port
  moveMotor(FORWARD, 40, 100);
  digitalWrite(s_dir, HIGH);
  step_prog(100);
  go_to_base(); // sends carrier back to base in case it does not start from there
```

```
  //Serial.println("Carrier is at base.");
  digitalWrite(sleep_pin, LOW); // sets the pololu (stepper driver) to sleep (HIGH wakes it up)
}
// the main loop reads the Serial monitor and asks for commands
void loop()
{
  Serial.read();
  start_command = Serial.parseInt();
  //Serial.println ("8 = Start; 9 = Go to Base; 4 = Single Move");
  while (Serial.available() == 0) {}//I am just waiting till somebody enters something!
  if (Serial.available() != 0)
  {
    start_command = Serial.parseInt();
    if (start_command == 0) // enables to type in coordinates of a tag on a paper and goes to
this position
    {
      Serial.println("1");
    }
    if (start_command == 4) // enables to type in coordinates of a tag on a paper and goes to
this position
    {
      random_move();
    }
    if (start_command == 5) // asks for a paper type and than goes to every single position of
the tags
    {
      stops();
      tag_sheet_program();
    }
    if (start_command == 9) // sends carriage back to base
    {
      go_to_base();
    }
  }
}

// enables typing in coordinates of a tag on a paper and goes to this position
int random_move()
{
  Serial.read(); //clears the Serial monitor
  Serial.println("Enter X:");
  while (Serial.available() == 0) {}//I am just waiting till somebody enters something!
  if (Serial.available() != 0)
  {
    x = Serial.parseInt();
    Serial.println(x);
  }
  Serial.read();
  Serial.println("Enter Y:");
  while (Serial.available() == 0) {
  }//I am just waiting till somebody enters something!
  if (Serial.available() != 0)
  {
    y = Serial.parseInt();
    Serial.println(y);
  }
  moveXY(x, y); // opens the moveXY function to move the carriage
}
// gets called by tag_sheet_program; moves the motors according to the coordinates
void moveXY(int x, int y) {
  if ((x > cur_x) && (y > cur_y)) // moves the Stepper motor and DC motor in positive direction
  {
    moveMotor(FORWARD, 40, (x - cur_x) / conv_x);
    digitalWrite(s_dir, HIGH);
    step_prog((y - cur_y) / conv_y);
    Serial.print("Current x step distance: ");
    Serial.print(abs(x));
```

```
    Serial.println(" mm");
    Serial.print("Current y step distance: ");
    Serial.print(abs(y));
    Serial.println(" mm");
  }
  if ((x == cur_x) && (y > cur_y)) // moves the Stepper motor in positive direction
  {
    digitalWrite(s_dir, HIGH);
    step_prog((y - cur_y) / conv_y);
    Serial.print("Current x step distance: ");
    Serial.print(abs(x));
    Serial.println(" mm");
    Serial.print("Current y step distance: ");
    Serial.print(abs(y));
    Serial.println(" mm");
  }
  if ((x < cur_x) && (y > cur_y)) // moves the stepper motor in positive and the DC in negative
direction
  {
    moveMotor(BACKWARD, 40, (cur_x - x) / conv_x);
    digitalWrite(s_dir, HIGH);
    step_prog((y - cur_y) / conv_y);
    Serial.print("Current x step distance: ");
    Serial.print(abs(x));
    Serial.println(" mm");
    Serial.print("Current y step distance: ");
    Serial.print(abs(y));
    Serial.println(" mm");
  }
  if ((x > cur_x) && (y < cur_y)) // moves the Stepper motor and DC motor in positive direction
  {
    moveMotor(FORWARD, 40, (x - cur_x) / conv_x);
    digitalWrite(s_dir, LOW);
    step_prog((cur_y - y) / conv_y);
    Serial.print("Current x step distance: ");
    Serial.print(abs(x));
    Serial.println(" mm");
    Serial.print("Current y step distance: ");
    Serial.print(abs(y));
    Serial.println(" mm");
  }
  if ((x == cur_x) && (y < cur_y)) // moves the Stepper motor in positive direction
  {
    digitalWrite(s_dir, LOW);
    step_prog((cur_y - y) / conv_y);
    Serial.print("Current x step distance: ");
    Serial.print(abs(x));
    Serial.println(" mm");
    Serial.print("Current y step distance: ");
    Serial.print(abs(y));
    Serial.println(" mm");
  }
  if ((x < cur_x) && (y < cur_y)) // moves the stepper motor in positive and the DC in negative
direction
  {
    moveMotor(BACKWARD, 40, (cur_x - x) / conv_x);
    digitalWrite(s_dir, LOW);
    step_prog((cur_y - y) / conv_y);
    Serial.print("Current x step distance: ");
    Serial.print(abs(x));
    Serial.println(" mm");
    Serial.print("Current y step distance: ");
    Serial.print(abs(y));
    Serial.println(" mm");
  }
  if ((x > cur_x) && (y == cur_y)) // moves the DC motor in positive direction
  {
```

```
    moveMotor(FORWARD, 40, (x - cur_x) / conv_x);
    Serial.print("Current x step distance: ");
    Serial.print(abs(x));
    Serial.println(" mm");
  }
  if ((x < cur_x) && (y == cur_y)) // moves the DC motor in negative direction
  {
    moveMotor(BACKWARD, 40, (cur_x - x) / conv_x);
    Serial.print("Current x step distance: ");
    Serial.print(abs(x));
    Serial.println(" mm");
  }
  if ((x == 0) && (y == 0)) // sends the carriage back to base
  {
    go_to_base();
  }
  cur_x = x; // saves the current position
  cur_y = y;
}

// this is the main function, which sends the position of the tag to the moveXY function; it
receives the positions
from stops();
void tag_sheet_program()
{
  detectState_x = digitalRead(encoderIn_x);
  detectState_y = digitalRead(encoderIn_y);
  if ((detectState_y == 1) && (detectState_x == 1)) // checks if the carrier is at the base; in
this case it goes to
    the position of the first tag, otherwise to the position of the second
  {
    moveMotor(FORWARD, 40, (pos_x[0]) / conv_x); // goes to the position of the first tag; this
is necessary to repeat
    the the movement for the same paper type
    digitalWrite(s_dir, HIGH);
    step_prog(pos_y[0] / conv_y);
    cur_x = pos_x[0];
    cur_y = pos_y[0];
    Serial.print("Current x step distance: ");
    Serial.print(abs(cur_x));
    Serial.println(" mm");
    Serial.print("Current y step distance: ");
    Serial.print(abs(cur_y));
    Serial.println(" mm");
  }
  Serial.println ("Please enter 5 to continue! OK CONTINUE"); // stops the program and waits for
a start command
  while (Serial.available() == 0 || Serial.parseInt() != wait_go) {
  }
  for (int i = 1; i < length; i++) // reads the position of the tags; starts at the second tag
  {
    moveXY(pos_x[i], pos_y[i]);
    Serial.println ("Please enter 5 to continue! OK CONTINUE"); // allows us to stop the program
and wait for
    a continue command
    while (Serial.available() == 0 || Serial.parseInt() != wait_go) {}
  }
  Serial.println("OK DONE");
  moveMotor(BACKWARD, 40, (pos_x[length - 1] - pos_x[0]) / conv_x); // sends the carriage back to
the position of the first
  tag
  digitalWrite(s_dir, LOW);
  step_prog((pos_y[length - 1] - pos_y[0]) / conv_y);
  cur_x = pos_x[0]; // this is important to tell the moveXY(); what the position of the carriage
is
  cur_y = pos_y[0];
  go_to_base();
```

```
}
// the following two functions are for the Stepper motor
void step_prog(int step_amount) // stepper function which allows it to enter the amount of steps,
the stepper
motor should go
{
  for (int a = 0; a < step_amount; a++)
  {
    single_step();
  }
}
void single_step() // this is the function for one single step
{
  digitalWrite(s_step, HIGH);
  delayMicroseconds(650);
  digitalWrite(s_step, LOW);
  delayMicroseconds(650);
}
// the following codes are for the DC motor
void moveMotor(int direction, int PWM_val, long tick) // main function, you call to move the
motor
{
  countInit = count; // abs(count)
  tickNumber = tick;
  if (direction == FORWARD) motorForward(PWM_val);
  else if (direction == BACKWARD) motorBackward(PWM_val);
}
void rencoder() { // pulse and direction, direct port reading to save cycles
  if (PINB & 0b00000001) count++; // if(digitalRead(encodPinB)==HIGH) count_r ++;
  else count--; // if (digitalRead(encodPinB)==LOW) count_r --;
  if (run)
    if ((abs(abs(count) - abs(countInit))) >= tickNumber) motorBrake();
}
void motorForward(int PWM_val) // moves the DC Motor forward
{
  analogWrite(PWM1, PWM_val);
  digitalWrite(Dir, LOW);
  run = true;
}
void motorBackward(int PWM_val) //moves the DC Motor backward
{
  analogWrite(PWM1, PWM_val);
  digitalWrite(Dir, HIGH);
  run = true;
}
void motorBrake() { // stops the DC motor and holds it
  analogWrite(PWM1, 0);
  run = false;
}
void go_to_base() // sends the carriage to the base
{
  detectState_x = digitalRead(encoderIn_x);
  detectState_y = digitalRead(encoderIn_y);
  while (detectState_x == 0 && detectState_y == 0)
  {
    moveMotor(BACKWARD, 40, 10);
    detectState_x = digitalRead(encoderIn_x);
    digitalWrite(s_dir, LOW);
    single_step();
    detectState_y = digitalRead(encoderIn_y);
  }
  while (detectState_x == 0)
  {
    moveMotor(BACKWARD, 40, 10);
    detectState_x = digitalRead(encoderIn_x);
  }
  while (detectState_y == 0)
```

```
  {
    digitalWrite(s_dir, LOW);
    single_step();
    detectState_y = digitalRead(encoderIn_y);
  }
  cur_x = 0;
  cur_y = 0;
  digitalWrite(sleep_pin, LOW);
  Serial.println("OK HOME");
}

int stops() // Asks for the papertype and reads the position of the tags into a pos_x and pos_y
array
{
  Serial.read();
  Serial.println("Select paper type:");
  Serial.println("Type 1: Some-tag 8 tags, xx mm distance"); // dogbone
  Serial.println("Type 2: Dogbone 9 tags, 40 mm distance");// dogbone
  Serial.println("Type 3: Dogbone 5 tags, 50 mm distance");// dogbone
  Serial.println("Type 4: Dogbone 5 tags, 40 mm distance");// dogbone
  Serial.println("Type 5: Alien Square 9 tags, 50 mm distance"); // Alien Square
  Serial.println("Type 6: Alien Square 9 tags, 40 mm distance"); // Alien Square
  Serial.println("Type 7: Alien Square 5 tags, 50 mm distance"); // Alien Square
  Serial.println("Type 8: Alien Square 5 tags, 40 mm distance"); // Alien Square
  while (Serial.available() == 0) {} //I am just waiting till somebody enters something!
  if (Serial.available() != 0)
  {
    num = Serial.parseInt();
    length = lengths[num - 1];
    switch (num)
    {
      case 1:
        for ( int j = 0; j < length; j++) // case 1 reads the first two rows of the pos array
        {
          pos_x[j] = pos[0][j];
          pos_y[j] = pos[1][j];
        }
        break;
      case 2:
        for ( int j = 0; j < length; j++) // case 2 reads the last two rows of the pos array
        {
          pos_x[j] = pos[2][j];
          pos_y[j] = pos[3][j];
        }
        break;
      case 3:
        for (int j = 0; j < length; j++) // case 2 reads the last two rows of the pos array
        {
          pos_x[j] = pos[4][j];
          pos_y[j] = pos[5][j];
        }
        break;
      case 4:
        for (int j = 0; j < length; j++) // case 2 reads the last two rows of the pos array
        {
          pos_x[j] = pos[6][j];
          pos_y[j] = pos[7][j];
        }
        break;
      case 5:
        for (int j = 0; j < length; j++) // case 1 reads the first two rows of the pos array
        {
          pos_x[j] = pos[8][j];
          pos_y[j] = pos[9][j];
        }
        break;
      case 6:
```

```
        for (int j = 0; j < length; j++) // case 2 reads the last two rows of the pos array
        {
          pos_x[j] = pos[10][j];
          pos_y[j] = pos[11][j];
        }
        break;
      case 7:
        for (int j = 0; j < length; j++) // case 2 reads the last two rows of the pos array
        {
          pos_x[j] = pos[12][j];
          pos_y[j] = pos[13][j];
        }
        break;
      case 8:
        for (int j = 0; j < length; j++) // case 2 reads the last two rows of the pos array
        {
          pos_x[j] = pos[14][j];
          pos_y[j] = pos[15][j];
        }
        break;
      default:
        Serial.println("Please re-enter a valid paper type!"); // if the number is wrong, it
repeats stops();
        Serial.println();
        stops();
        break;
    }
  }
}
//END
////////////////////////////////////////////////////////////////////////////////////////////
///////
```

C# GUI for communicating with reader and collecting data

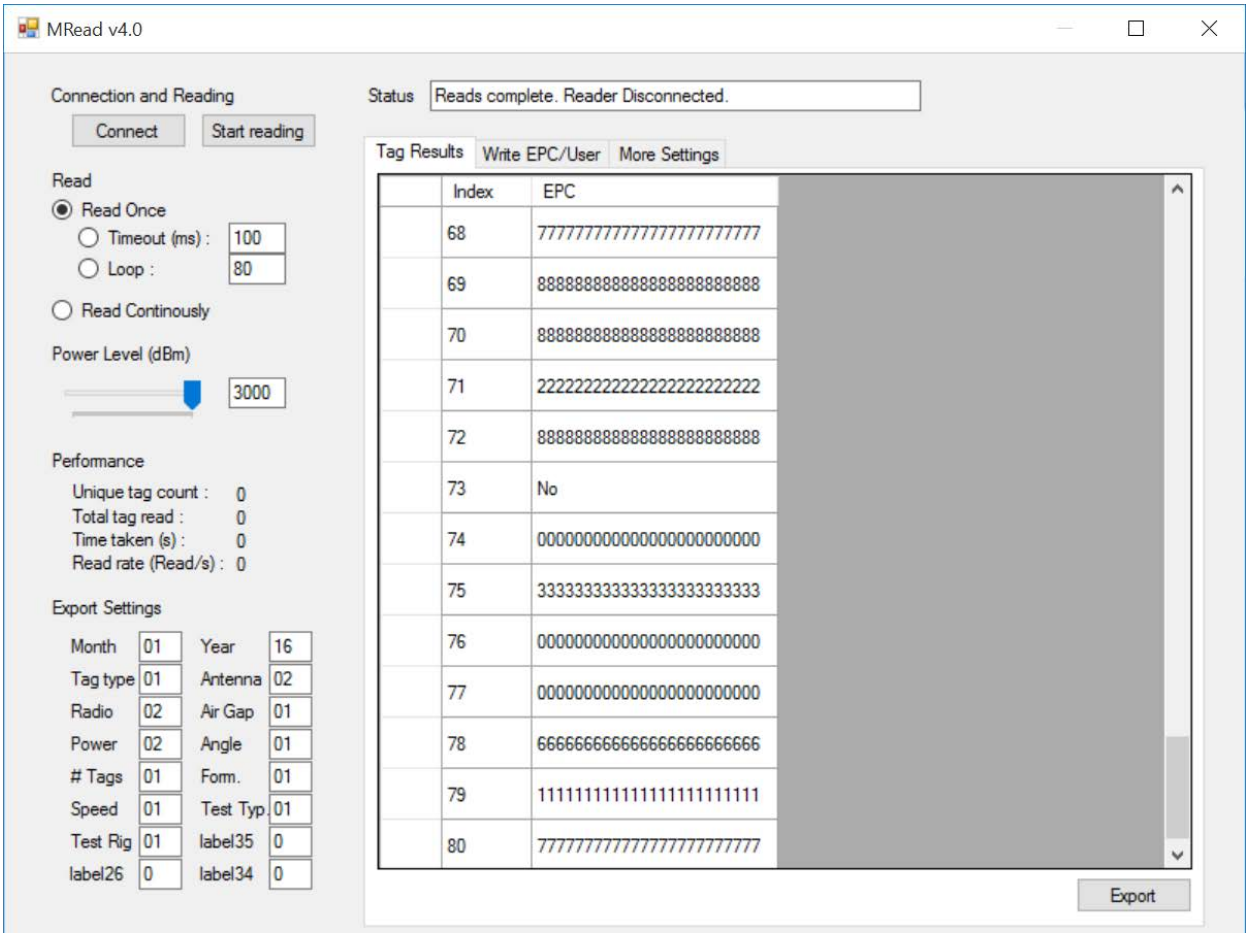

“Read Type” and “Power Level” can be adjusted to according to experimental conditions.
“Status” bar will show the connection to the reader and operation status.
First tab, “Tag Results”, shows the information of the tags detected by the radio.

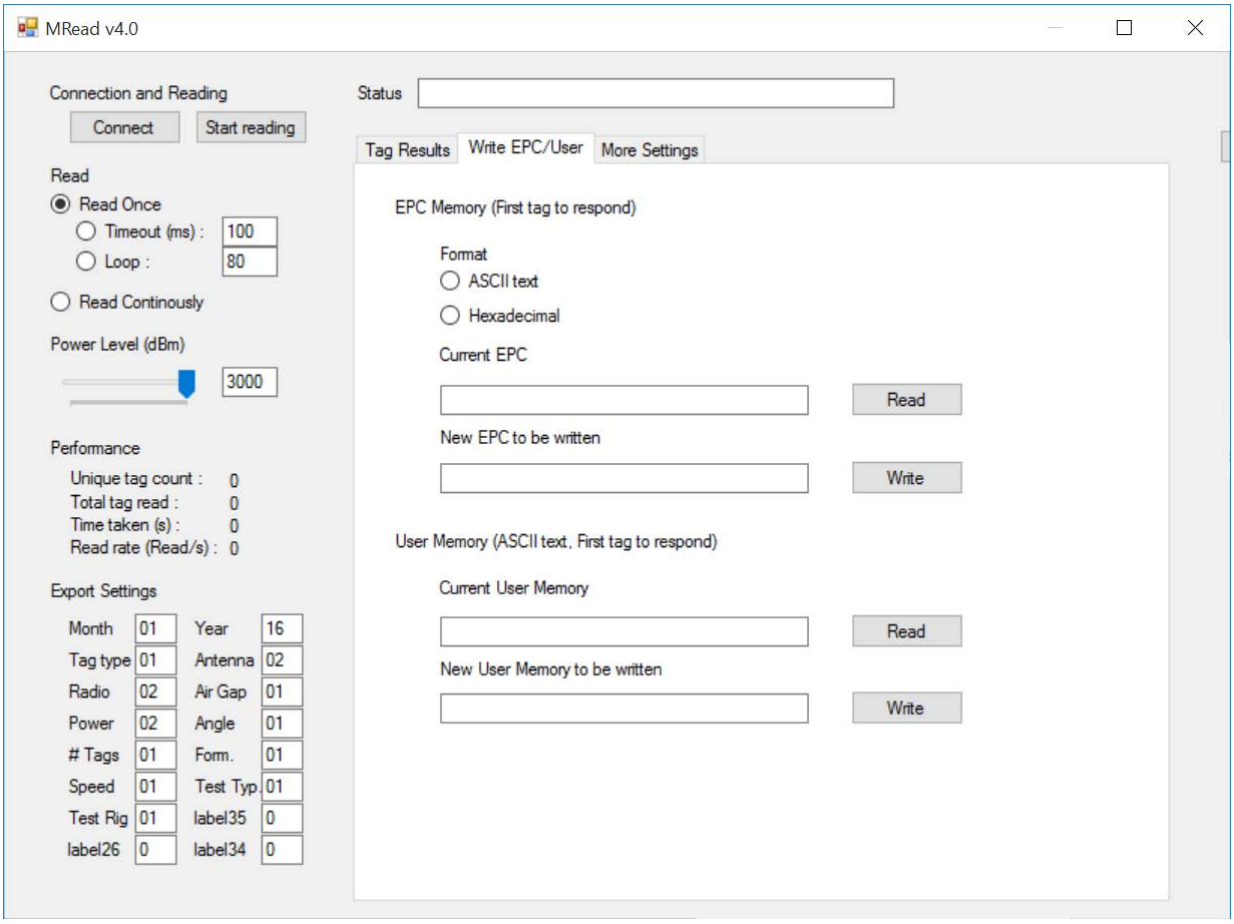

Second tab, “Write EPC/user”, enables the writing to the RFID tags, not optimized for experimental write operation.

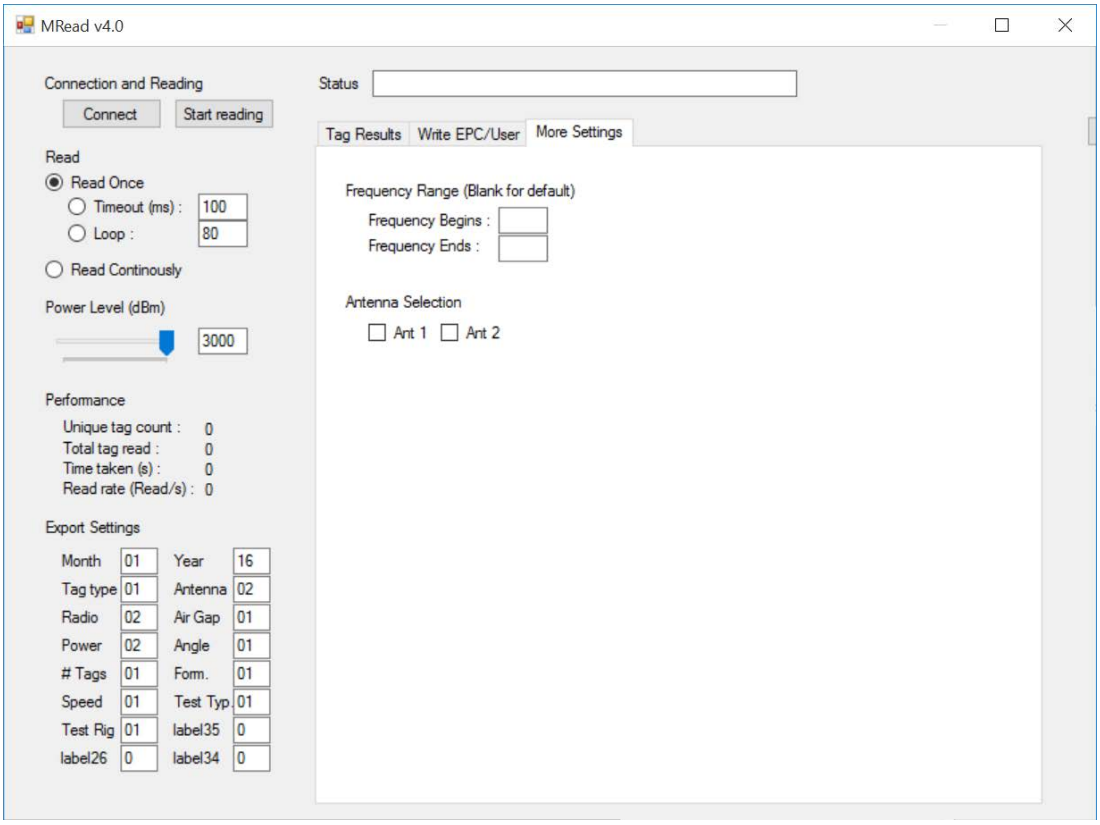

Third tab, “More Settings”, enables and disables the frequency hopping of the radio in the UHF band.

Bibliography

[1] P. Ali-Rantala et al. "Different Kinds of Walls And Their Effect on The Attenuation of Radiowaves Indoors". In: *Antennas and Propagation Society International Symposium*. Vol. 3. 1020-1023. June 2003.

[2] Larry B. Barrentine. *An Introduction to Design of Experiments*. Vol. 114. ASQ Quality Press, 1999. ISBN: 9780873894449.

[3] M. S. R. Bashri, M. I. Ibrahimy, and S. M. A. Motakabber. "A planar wideband microstrip patch antenna for UHF RFID tag". In: *2013 IEEE International Conference on Space Science and Communication (IconSpace)*. July 2013, pp. 302–306. DOI: 10.1109/IconSpace.2013.6599485.

[4] Gary Breed. "Basic Principles of Electrically Small Antennas". In: *High Frequency Electronics* (Feb. 2007), pp. 50–52.

[5] Gary Breed. "The Fundamentals of Patch Antenna Design and Performance". In: *High Frequency Electronics* (Mar. 2009), pp. 48–51.

[6] D.M. Dobkin. *The RF in RFID: UHF RFID in Practice*. Elsevier Science, 2012. ISBN: 9780123948304. URL: https://books.google.com/books?id=qiEieFBtdd4C.

[7] D.M. Dobkin and S.M. Weigand. "Environmental effects on RFID tag antennas". In: *Microwave Symposium Digest, 2005 IEEE MTT-S International*. June 2005. DOI: 10.1109/MWSYM.2005.1516541.

[8] Rich Fletcher, Uttara P. Marti, and Rich Redemske. "Study Of UHF RFID Signal Propagation Through Complex Media". In: *IEEE* 1B (2005), pp. 747–750.

[9] F. Fuschini et al. "Electromagnetic Analyses of Near Field UHF RFID Systems". In: *IEEE Transactions on Antennas and Propagation* 58.5 (May 2010), pp. 1759–1770. ISSN: 0018-926X. DOI: 10.1109/TAP.2010.2044328.

[10] F. Fuschini et al. "Electromagnetic Analyses of Near Field UHF RFID Systems". In: *IEEE Transactions on Antennas and Propagation* 58.5 (May 2010), pp. 1759–1770. ISSN: 0018-926X. DOI: 10.1109/TAP.2010.2044328.

[11] Robert Gallager. "Principles of Digital Communications". 2006. URL: http://ocw.mit.edu/courses/electrical-engineering-and-computer-science/6-450-principles-of-digital-communications-i-fall-2006/lecture-notes/book_1.pdf.

[12] J. Z. Huang et al. "A compact broadband patch antenna for UHF RFID tags". In: *2009 Asia Pacific Microwave Conference*. Dec. 2009, pp. 1044–1047. DOI: 10.1109/APMC.2009.5384364.

[13] J. Landt. "The History of RFID". In: *Potentials, IEEE* 24.4 (Oct. 2005), pp. 8–11. ISSN: 0278-6648. DOI: 10.1109/MP.2005.1549751.

[14] M. Laniel, I. Uysal, and J. P. Emond. "Radio Frequency Interactions With Air Cargo Container Materials For Realtime Cold Chain Monitoring". In: *AGRIS* 24.4 (2014), pp. 647–652.

[15] Magalie Laniel, Ultan Mc Carthy, and Ismail Uysal. "An RFID Perspective". In: Academy Publish, 2014. Chap. Wave Propagation, pp. 585–604. URL: http://www.academypublish.org/paper/wave-propagation:-an-rfid-perspective.

[16] Hong Mei Li et al. "Influence Of UHF Tags In The Different Materials Surface To Rfid System". In: *IEEE APCAP* (2014).

[17] K. Lum. "Experimental Investigation of the Key Factors that Affect the Programming Efficacy of Passive UHF RFID tags". MA thesis. University of Kentucky, 2012.

[18] K Lum et al. "Experimental Investigation and Numerical Optimization of Key Factors Affecting the Programming Efficacy of Passive UHF RFID Tags". In: *ASME International Mechanical Engineering Congress and Exposition, San Diego*. 2013.

[19] Arun N. Nambiar. "RFID Technology: A Review of its Applications". In: *WCECS* 2 (Oct. 2009).

[20] E.W.T. Ngai et al. "RFID research: An academic literature review (1995–2005) and future research directions". In: *International Journal of Production Economics* 112.2 (2008), pp. 510–520. ISSN: 0925-5273. DOI: http://dx.doi.org/10.1016/j.ijpe.2007.05.004. URL: http://www.sciencedirect.com/science/article/pii/S0925527307001934.

[21] Pavel Nikitin. "Leon Theremin (Lev Termen)". In: *Antennas and Propagation Magazine, IEEE* 54.5 (2012), pp. 252–257.

[22] P.V. Nikitin, K.V.S. Rao, and S. Lazar. "An Overview of Near Field UHF RFID". In: *RFID, 2007. IEEE International Conference on RFID*. Mar. 2007, pp. 167–174. DOI: 10.1109/RFID.2007.346165.

[23] D. Proffitt. "Experimental Investigation To Inform Optimal Configurations For Dynamic Near-Field Passive UHF RFID Systems". MA thesis. University of Kentucky, 2013.

[24] Xianming Qing and Zhi Ning Chen. "Proximity Effect Of Metallic Environments On High Frequency RFID Antenna: Study And Applications". In: *IEEE* (2007).

[25] K. V. S. Rao, Pavel V. Nikitin, and Sander F. Lam. "Impedance Matching Concepts in RFID Transponder Design". In: *IEEE* (Oct. 2005), pp. 39–42. DOI: http://dx.doi.org/10.1109/AUTOID.2005.35.

[26] A. Ren et al. "A Robust UHF Near-Field RFID Reader Antenna". In: *IEEE Transactions on Antennas and Propagation* 60.4 (Apr. 2012), pp. 1690–1697. ISSN: 0018-926X. DOI: 10.1109/TAP.2012.2186254.

[27] Mark Roberti. "The History of RFID Technology". In: *RFID Journal* (Jan. 2005). URL: http://www.rfidjournal.com/articles/pdf?1338.

[28] James Jungbae Roh, Anand Kunnathur, and Monideepa Tarafdar. "Classification of RFID adoption: An expected benefits approach". In: *Information and Management* 46 (July 2009), pp. 357–363.

[29] Patrick L. Ryan. "Radio Frequency Propagation Differences Through Various Transmissive Materials". MA thesis. University Of North Texas, Dec. 2002.

[30] Shuai Shao, R.J. Burkholder, and J.L. Volakis. "Physics-based Approach for Antenna Design Optimization of RFID Tags Mounted On and Inside Material Layers". In: *Antennas and Propagation Society International Symposium (APSURSI), 2014 IEEE*. July 2014, pp. 1676–1677. DOI: 10.1109/APS.2014.6905164.

[31] L. Shen et al. "A Yagi-Uda Antenna with Load and Additional Reflector for Near-field UHF RFID". In: *IEEE Antennas and Wireless Propagation Letters* PP.99 (2016), pp. 1–1. ISSN: 1536-1225. DOI: 10.1109/LAWP.2016.2601115.

[32] Claire Swedberg. *Sales of EPC RFID Tags, ICs Reach Record Levels*. Tech. rep. RFID Journal, 2010. URL: http://www.rfidjournal.com/articles/pdf?7952.

[33] Harald Vogt. "Efficient Object Identification with Passive RFID Tags". In: *Springer* 2414 (Aug. 2002), pp. 98–113.

[34] R. Want. "An introduction to RFID technology". In: *Pervasive Computing, IEEE* 5.1 (Jan. 2006), pp. 25–33. ISSN: 1536-1268. DOI: 10.1109/MPRV.2006.2.

[35] Li Da Xu, Wu He, and Shancang Li. "Internet of Things in Industries: A Survey". In: *Industrial Informatics, IEEE Transactions on* 10.4 (Nov. 2014), pp. 2233–2243. ISSN: 1551-3203. DOI: 10.1109/TII.2014.2300753.

Vita

Zi Qin Phua, an international student from Malaysia, received his bachelor's degree of Mechanical Engineering at University of Kentucky in 2013. He decided to pursue an advanced degree in the field of RFID systems at University of Kentucky. He is expected to receive his master's degree in May 2017.